Article type   : Original Article

Interactions between Transport Protein Particle (TRAPP) complexes and Rab GTPases in Arabidopsis

Monika Kalde[1#], Liam Elliott[1#]*, Raksha Ravikumar[2#], Katarzyna Rybak[2], Melina Altmann[3], Susan Klaeger[4], Christian Wiese[2], Miriam Abele[2], Benjamin Al[2], Nils Kalbfuß[2], Xingyun Qi[5], Alexander Steiner[2], Chen Meng[6], Huanquan Zheng[5], Bernhard Kuster[4], Pascal Falter-Braun[3,7], Christina Ludwig[6], Ian Moore[1§], Farhah F. Assaad[2§]*

#: these authors contributed equally

§: co-last.

*: corresponding authors.

[1] Department of Plant Sciences, University of Oxford, Oxford OX1 3RB, United Kingdom

[2] Plant Science Department, Botany, Technische Universität München, 85354 Freising, Germany

[3] Institute of Network Biology (INET), Helmholtz Zentrum München, Deutsches Forschungszentrum für Gesundheit und Umwelt (GmbH), 85764 Neuherberg, Germany

[4] Chair of Proteomics and Bioanalytics, Technische Universität München, 85354 Freising, Germany

[5] Department of Biology, McGill University, Montreal, H3B 1A1 Canada

[6] BayBioMS, Bavarian Center for Biomolecular Mass Spectrometry, Technische
Universität München, 85354 Freising, Germany

[7] Faculty of Biology, Microbe-Host-Interactions, Ludwig-Maximilians-Universität (LMU)
München, 82152 Planegg-Martinsried, Germany

* corresponding author

Botany

Plant Science Department

Technische Universität München

Emil-Ramann-Str. 4

85354 Freising

Germany

Farhah@wzw.tum.de

Tel: +49-8161-71-5437

FAX: +49-8161-71-5432

Summary

The Transport Protein Particle II (TRAPPII) is essential for exocytosis, endocytosis,
protein sorting and cytokinesis. In spite of a considerable understanding of its biological
role, little is known about Arabidopsis TRAPPII complex topology and molecular function.
In this study, independent proteomic approaches initiated with TRAPP components or
Rab-A GTPase variants converge on the TRAPPII complex. We show that the
Arabidopsis genome encodes the full complement of 13 TRAPPC subunits, including four
previously unidentified components. A dimerization model is proposed to account for
binary interactions between TRAPPII subunits. Preferential binding to dominant negative

(GDP-bound) versus wild-type or constitutively active (GTP-bound) RAB-A2a variants discriminates between TRAPPII and TRAPPIII subunits and shows that Arabidopsis complexes differ from yeast but resemble metazoan TRAPP complexes. Analyses of Rab-A mutant variants in *trappii* backgrounds provide genetic evidence that TRAPPII functions upstream of RAB-A2a, allowing us to propose that TRAPPII likely behaves as a Guanine-nucleotide Exchange Factor (GEF) for the RAB-A2a GTPase. GEFs catalyze exchange of GDP for GTP; the GTP-bound, activated, Rab then recruits a diverse local network of Rab effectors to specify membrane identity in subsequent vesicle fusion events. Understanding GEF-Rab interactions will be crucial to unraveling the co-ordination of plant membrane traffic.

Introduction

Membrane traffic is central to the organisation of eukaryotic cells. It provides essential biosynthetic and degradative functions via secretion, membrane biogenesis, endocytosis, vacuolar expansion, vacuolar degradation, and autophagy. In plant cells major sorting decisions that target macromolecules towards biosynthetic versus degradative pathways occur at the *trans*-Golgi Network/Early Endosome (TGN/EE), which has emerged as a central hub for membrane traffic during interphase and cytokinesis (Dettmer et al., 2006; Chow et al., 2008; Ravikumar et al., 2018). The TGN/EE may be homologous to the metazoan recycling endosome and yeast post-Golgi endosome, though it is likely that it has unique characteristics of its own. Indeed, localisation studies indicate that it has at least two distinct functional domains (Dettmer et al., 2006; Chow et al., 2008; Ravikumar et al., 2018). During cell division, one of these domains forms the cell plate (Chow et al., 2008; Ravikumar et al., 2018), a structure unique to plant cytokinesis. The plant TGN/EE has essential functions in exocytosis, endocytosis and protein sorting as well as a number of specialized functions such as cell plate formation in dividing cells (Luo et al., 2015; Rosquette et al., 2018; Ravikumar et al., 2018). In Arabidopsis, all of these functions are, at least in part, mediated by the Transport Protein Particle II (TRAPPII) complex. Arabidopsis TRAPPII null mutants are seedling lethal and have severe cytokinesis defects as well as profound loss of cell polarity (Jaber et al., 2010; Thellmann et al., 2010; Qi et al., 2011; Rybak et al., 2014; Zhang et al., 2018; Ravikumar et al., 2018), consistent with the central role of TGN/EE trafficking in plant cell organisation. In spite of its pivotally important biological role, little is known about Arabidopsis TRAPPII complex topology and molecular function.

In 2016, four modular TRAPP complexes (TRAPPI to TRAPPIV) were reported in yeast (Lipatova et al., 2016). However, the existence of TRAPPI and TRAPPIV has since been contested. Indeed, protein purification at the lowest salt concentration that allows for the release of TRAPP subunits from membranes has uncovered only two TRAPP complexes, TRAPPII and TRAPPIII, in yeast cells (Thomas et al., 2018). These two complexes share six common subunits, which are combined with complex-specific subunits in a modular fashion to form the different complexes. TRAPPII-specific subunits in yeast are Tca17, Trs65, Trs120 and Trs130 (Thomas et al., 2018). TRAPPIII consists of the six common subunits combined with a single complex-specific subunit, Trs85. In metazoans, only two complexes, TRAPPII and TRAPPIII, are known and their subunit composition differs from those of their yeast counterparts (Riedel et al., 2018; Sacher et al., 2018). In plants, the subunit composition and modularity of TRAPP complexes remain to be determined. Furthermore, it is unclear whether Arabidopsis TRAPPII more closely resembles yeast or metazoan orthologous complexes.

In yeast and mammals, the best documented function of TRAPP complexes is to act as Guanine-nucleotide Exchange Factors (GEFs) for Rab GTPases. Rab GTPases are critical self-organising determinants of membrane identity that ensure accurate and efficient membrane trafficking between compartments (Barr, 2013). Individual members of the Rab GTPase family are recruited from the cytosol onto particular membrane domains where they are activated by specific GEFs. GEFs catalyse the removal of GDP from Rab GTPases, which allows for the subsequent binding of GTP. The GTP-bound, activated Rab then recruits a diverse local network of Rab effectors to the membrane. Effectors typically include tethering factors, for membrane-membrane recognition, as well as the GEF for the next Rab GTPase in the pathway. Such 'Rab cascades', in which one Rab GTPase recruits the next, are crucial for the spatiotemporal self-organisation of membrane identity and sorting.

The requirement for sorting cargoes into diverse trafficking pathways at the TGN/EE may explain the diversity of TGN/EE or post-Golgi Rab GTPases in plant cells. The Rab GTPase clade that acts principally at the TGN/EE, the Rab-A clade (related to Ypt3 in *Saccharomyces pombe*, Ypt31-32 in *Saccharomyces cerevisiae* and Rab11 of metazoans), has undergone a unique and extraordinary diversification in land plants (Rutherford and Moore, 2002). A single ancestral gene in charophyte ancestors diversified progressively into 26 genes; these fall into 6 putative Rab subclasses (Rab-A1 to –A6) that are widely conserved across angiosperm genomes. The question arises as to how these 26 Rab-A GTPases are differentially activated. In both yeast and mammals, TRAPPII complexes have been shown to exhibit Ypt31-32/Rab-11 GEF activity

(Morozova et al., 2006; Riedel et al., 2018). Furthermore, the TGN/EE-localisation of TRAPPII components makes the TRAPPII complex a promising candidate for a Rab-A GEF in plants (Qi and Zheng, 2011; Nakano et al., 2014; Ravikumar et al., 2017; Ravikumar et al., 2018). The TRAPPII complex has, in fact, been functionally linked to the Rab-A1 subclade, but the nature of this link remains unclear (Qi et al., 2011; Qi and Zheng, 2011). Whilst plant Rab GEFs are known for the Rab-G (Cui et al., 2014) and Rab-F clades (Goh et al., 2007; Fukuda et al., 2013) and possible GEFs have been suggested for the Rab-E and Rab-H clades (Mayers et al., 2017; Jia et al., 2018) the only evidence that Arabidopsis TRAPPII acts as a GEF is based on the partial suppression of a *trappii* null allele by a constitutively active Rab-A1 GTPase, ectopically expressed from a strong promotor (Qi et al., 2011; Qi and Zheng, 2011).

Given the diversity of Rab-A GTPases in plant cells, together with the potential diversity of trafficking functions at the TGN/EE, Golgi, or autophagosome, TRAPP and Rab functions cannot be reliably inferred via orthology but need to be established experimentally in plants. In this study, we elucidate the subunit composition of Arabidopsis TRAPP complexes, pointing to the existence of a distinct TRAPPIII complex containing subunits not previously recognised in plant genomes. Our data also present multiple lines of evidence for the role of TRAPPII as a putative GEF for Rab-A2.

Results

The Arabidopsis proteome contains the full complement of known TRAPP subunits

Thus far, only 9 of 13 potential TRAPP subunits have been identified by homology in plant genomes (Thellmann et al., 2010; Paul et al., 2014) and of these only 6 have been identified in immunoprecipitated TRAPPII complexes (Rybak et al., 2014, see BIOGRID; Steiner et al., 2016). TRAPP subunits have also been detected in the interactome of a TGN/EE-associated t-SNARE, SYP61 (Drakakaki et al., 2012). Our first aim was to identify further TRAPP homologues. To this end, we carried out immunoprecipitation experiments with mass spectrometry readout (IP-MS). The TRAPPII-specific CLUB/AtTRS130:GFP subunit, expressed in stable transgenic Arabidopsis plants, was used as bait. This approach uncovered homologues of all known TRAPP subunits (Table I; Fig. S1), with the exception of Trs23/TRAPPC4, a subunit common to both yeast and metazoan TRAPPII and TRAPPIII. TRAPP subunits found in CLUB/AtTRS130 IPs included four subunits (TRAPPC2(C2L), TRAPPC11, TRAPPC12, TRS65/TRAPPC13)

not previously recognized in plant genomes due to low conservation with yeast sequences. While the full complement of thirteen known TRAPP subunits was detected in CLUB IP-MS, nine of these were high confidence interactors (intensity ratio > 8 and P < 0.02; black in Table I), one was of intermediate rank (intensity ratio < 8 and P < 0.02; green in Table I), and three subunits failed to meet our significance cutoffs (P > 0.02; red in Table I). TRS65/TRAPPC13, which is a TRAPPII subunit in yeast but a TRAPPIII subunit in metazoans, had an intermediate intensity ratio of 7. 3 (Table I; Fig. S1). The high confidence interactors included shared and TRAPPII-specific subunits; the three TRAPP proteins that failed to meet our significance cutoff are homologues of metazoan TRAPPIII (Table I; Fig. S1).

Proteomic and binary interaction data support a dimerized structure for Arabidopsis TRAPPII

Yeast Two-Hybrid (Y2H) analyses were performed to test for binary interactions between TRAPPII components. CLUB/AtTRS130 and AtTRS120 TRAPPII truncations were designed via phylogenetic analysis, with highly conserved (C1, T1), intermediate or mixed (C2, T2) and plant-specific (C3, T3) moieties (Fig. 1a). With the exception of the CLUB_C1 truncation, all TRAPPII truncations and catalytic core subunits used as DB clones in pair-wise tests yielded at least one positive interaction (Fig. 1; Fig. S2) and this was used as an internal positive control for the interpretation of negative interaction data. An attempt at elucidating complex topology based on binary interaction data shows that interactions between the lower molecular weight Arabidopsis TRAPP subunits (BET3, BET5, TRS23, TRS31, TCA17 and TRS33) are entirely consistent with the crystal structure of yeast TRAPP core- or sub-complexes (Fig. 1b; Fig. S2; Kim et al., 2006). Our proposed structure (Fig. 1c) is also consistent with the rank of the TRAPP subunits in the IP-MS experiments (Table I) in that interactors with the highest absolute (Fig. S1) or relative (Table I) ranks are either binary interactors (i.e. TCA17) or one step removed in the complex (i.e. BET3 and TRS33). The plant-specific or less conserved moieties of the two TRAPPII-specific subunits strongly interact with each other (Fig. 1b; Fig. S2). In addition, the two extremities of AtTRS120 have a binary interaction in yeast (Fig. 1b; Fig. S2). A dimerization model is proposed to account for all these interactions (Fig. 1c), and this is similar to one of four dimerization models proposed, based on cryo-TEM imaging, by Taussig et al., 2013.

Genetic interaction data establish a functional link between the catalytic core and a *trappii*-specific allele

In the proposed dimerized model, each TRAPPII monomeric complex consists of a central catalytic core and of a large TRAPPII-specific moiety (Fig. 1c). To establish a functional link between these two moieties, we conducted double mutant analysis between a shared catalytic core and a *trappii*-specific allele. We focused on AtTRS33, a shared component of TRAPPII and TRAPPIII in yeast and metazoans (Lipatova et al., 2016; Thomas et al., 2018), because its homologue is implicated in TRAPPII assembly in yeast (Tokarev et al., 2009). We had previously characterized a null insertion allele, *trs33-1* (Thellmann et al., 2010), and this was crossed to a null allele of the TRAPPII-specific subunit CLUB/AtTRS130 (designated *club-2* in Jaber et al., 2010 and *trs130-1* Qi et al., 2011). To examine possible genetic interactions between *trs33-1* and *club-2*, we attempted to isolate the double mutant. We, however, failed to obtain any seedlings that were double homozygous for null mutants of these genes, indicating that *club-2 trs33-1* double mutants are either gametophytic or embryo lethal. We then monitored embryo phenotypes. Compared to single mutants of *club-2* or *trs33-1*, lines segregating both *club-2* and *trs33-1* exhibited abnormally developing embryos until the heart stage; these putative double mutant embryos remained globular and failed to acquire the heart shaped form (Fig. 2). The incidence of putative double mutants dropped from 8-15% at the globular (n = 234) and heart (n = 327; Fig. S3) stages to 0% by the torpedo stage (n = 155; Fig. S3). Taken together, we inferred that double mutant embryos are lethal, collapsing by the late heart stage. As *trs33-1* has a weak and *club-2* a moderate seedling lethal phenotype (as compared to *keule* and especially *knolle*, described by Assaad et al., 1996; Söllner et al., 2002; Jaber et al., 2010; Thellmann et al., 2010), we would expect an additive phenotype to correspond to strong seedling lethality and not to embryo lethality. Thus, our interpretation of embryo lethality is that this translates into a synergistic genetic interaction (Perez-Perez et al., 2009; Guarente, 1993). In conclusion, our genetic interaction data appears to establish a functional link between AtTRS33 and CLUB/AtTRS130, which complements the physical interaction data that attributes both proteins to the same complex.

Clade A, B, D and E Rab-GTPases are identified in the TRAPPII interactome

Following the above characterization of Arabidopsis TRAPPII subunits, we sought to use our proteomic analysis of CLUB/AtTRS130 to identify possible functional interactors of TRAPPII. TRAPPII complexes are thought to act as Rab GEFs in yeast and metazoans.

Accordingly, we scanned the CLUB/AtTRS130-GFP interactome for the presence of Rab GTPases. We found Rab-GTPases from the A clade, but also Rab GTPases in the B, D, and E clades (Table II; Fig. S1; Fig. S4). All four clades are on biosynthetic trafficking routes. Indeed, Rab-D GTPases are known to be required for ER to Golgi traffic, Rab-Bs for intra-Golgi transport, Rab-As for post-Golgi trafficking and TGN/EE function (Woodlard and Moore, 2008) and Rab-E GTPases are believed to function in traffic between the Golgi and plasma membrane (Zheng et al., 2005; Camacho et al., 2009; Speth et al., 2009; Ahn et al., 2013). Rab GTPases in all four clades had intermediate intensities in our IP-MS data (intensity ratio in the 5 – 8 range; Fig. S1), possibly owing to indirect binding to the CLUB bait via the shared catalytic core (see asterisk in Fig. 1c). The identification of Rab GTPases from four different clades in IP-MS with a TRAPPII-specific subunit may appear surprising. The trivial explanation, which is that these are false positives, is challenged by the observation that the Rab-GTPases listed in Table II passed all filters and cutoffs in our analyses (false discovery rate < 0.01, P value < 0.02, at least four peptides; see Experimental Procedures). However, the mere presence of a protein in IP-MS does not provide any information as to biological relevance, nor as to whether the TRAPPII bait acts as an upstream activator or as a downstream effector of the interacting Rab GTPase.

Quantitative co-IP with mass-spectrometry readout provides evidence for TRAPPII acting as a GEF for the Rab-A2 subclass.

According to classical models of Rab GTPase function, GDP-bound Rab GTPases are expected to interact preferentially with Rab GEFs, thereby allowing Rab activation through GDP displacement (Barr, 2013). The resulting GTP-bound (activated) Rab can then interact with Rab effectors. Multiple members of the Rab-A clade of plant Rab GTPases have been, like TRAPPII, implicated in cytokinesis in Arabidopsis (Chow et al., 2008; Qi & Zheng, 2013; Kirchhelle et al., 2016) and TRAPPII has been shown to be functionally linked to at least one Rab-A GTPase (Qi et al., 2011; Qi & Zheng, 2011). The Rab-A GTPase RAB-A2a is commonly used as a marker of the TGN/EE and the cell plate, and is known to be required for proper cytokinesis (Chow et al., 2008). Despite this, little is known as to the actual function of RAB-A2a during cytokinesis or in interphase cells, and no interactors of this GTPase have been reported. Following the identification of RAB-A2a in our TRAPPII interactome (Table II, Fig. S1, Fig. S4), we further investigated the possibility of a functional connection between RAB-A2a and TRAPPII, and that TRAPPII may be a RAB-A2 GEF. To identify potential GEFs of RAB-

A2a we used Rab proteins carrying defined amino acid substitutions that stabilize either the GDP- or GTP-bound form of the protein. GDP-bound or nucleotide-free variants of both Ras and Rab GTPases have previously been shown to interact preferentially with GEFs over wild-type and GTP-bound variants (Lai et al., 1993; Day et al., 1998; Goh et al., 2007). Conversely, Rab GTPase Activating Proteins and downstream effectors have been shown in some cases to preferentially interact with GTP-bound Rab variants (Vogel et al., 1998; Preuss et al., 2006; Camacho et al., 2009). We, therefore, employed a differential IP-MS protocol with GDP- versus GTP-bound RAB-A2a mutant variants in order to further investigate whether the TRAPPII complex could be a GEF for RAB-A2a. Rab GTPase SN mutants are predicted to favour GDP binding and expression of RAB-A2a[S26N] is known to produce a dominant-negative phenotype (Chow et al., 2008). We refer to YFP-tagged RAB-A2a[S26N] as YFP:A2a-DN below. The [Q71L] substitution of RAB-A2a[Q71L] has been shown in other Rab GTPases to reduce Rab GTP hydrolysis (Olkkonen & Stenmark, 1997; Ueda et al., 2001; Sohn et al., 2003; Chow et al., 2008) and such mutants are often considered to be constitutively active and GTP-bound. Hereafter, RAB-A2a[Q71L] will be referred to as YFP:A2a-CA (Chow et al., 2008).

A quantitative IP-MS protocol was developed to identify specific interactors of *Arabidopsis* Rab GTPases in detergent solubilised microsomes. The abundance of individual proteins was compared in triplicate replicates between total microsomes and co-IPs with YFP:RAB-A2a (TGN/EE localised; Chow et al., 2008) and the distantly related YFP:RAB-G3f that localises to the tonoplast and pre-vacuolar membranes (Geldner et al., 2009). Importantly, the proteins that co-purified with YFP:RAB-A2a and/or YFP:RAB-G3f included homologues of all 13 yeast or metazoan TRAPP subunits, including AtTRS23 (which was not detected in CLUB IP-MS) and the 4 previously unidentified subunits that were also detected in CLUB IP-MS (Tables III and IV, Fig. 3, Fig. S5, compare to Table I). *Arabidopsis* TRAPP subunits could be clearly divided into two distinct groups based on their relative interaction with the DN or CA forms of YFP:RAB-A2a, or by their preferential binding to YFP:RAB-A2a versus YFP:RAB-G3f (Tables III - V; Fig. 3). A first set of TRAPP subunits (colored green in Table V) preferentially bound to YFP:A2a-DN over both the wild-type YFP:A2a or YFP:A2a-CA variants, as can be seen by positive values in the direct comparisons in Table V. After the RAB-A2a bait itself, this first set of TRAPP subunits belonged to the top 10 interactors in the YFP:A2a-DN IPs. An additional characteristic of this set was preferential binding to RAB-A2a over RAB-G3f (as seen by negative values in the G3f/A2a column in Table IV; Fig. 3). This set of subunits closely matches the composition

of metazoan TRAPPII (Table V; green). This provides evidence for TRAPPII acting as a putative GEF for the Rab-A2 subclass at the plant TGN/EE.

The second set of *Arabidopsis* TRAPP subunits in the RAB-A2a interactor list were distinguished from TRAPPII by their failure to interact with YFP:A2a-DN (Table V, orange). This set of subunits may therefore interact with RAB-A2a as effectors rather than as a GEF. It closely matched the composition of metazoan TRAPPIII, including three subunits not present in yeast TRAPPIII and not previously recognised in plant genomes (see Table I). These subunits were all significantly (P < 0.001) enriched in the vacuolar YFP:RAB-G3f IP-MS and two of these preferentially bound to RAB-G3f over RAB-A2a (positive values in Table IV), perhaps reflecting a function for this complex in targeting to the vacuole. These observations provide prima facie evidence for the existence of a hitherto undescribed Arabidopsis TRAPPIII complex that contributes to vacuolar targeting and/or autophagy. Overall, the differential IP-MS strategy discriminates between two sets of TRAPP subunits, one of which, in pairwise comparisons, behaves like the TGN/EE-associated RAB-A2a whereas the other behaves like the vacuolar RAB-G3f.

YFP:RAB-A2a localisation dynamics are impaired in *trappii* mutants

RAB-A2a and TRAPPII have both previously been implicated in cytokinesis (Chow et al., 2008; Qi et al., 2011; Rybak et al., 2014). To assess the extent of their co-localisation during cell plate formation and maturation, we carried out live imaging with YFP:RAB-A2a (Chow et al., 2008) and TRS120:mCherry during cytokinesis (Rybak et al., 2014). The two markers co-localize at the cell plate throughout cytokinesis, with both markers reorganizing to the leading edges of the cell plate at telophase (Fig. 4a). This re-localisation of RAB-A2a and AtTRS120 during cell plate expansion is presumably a reflection of the fact that new membrane delivery is confined to the leading edge as the phragmoplast expands. In seedling lethal, null *trappii* mutants, YFP:RAB-A2a was recruited to the cell plate, but, in contrast to the wild type, it also labelled endosomal (or FM4-64 positive compartments) compartments in the vicinity of the cell plate (Fig. 4b,c ; Fig. S7a). During cell plate expansion and insertion, re-organisation of YFP:RAB-A2a to the leading edges of the cell plate was impaired (Fig. 4b,c ; Fig. S7). It is noteworthy that YFP:RAB-A2a retained membrane association in *trappii* mutants (Fig. 4b, 4c). The data show that TRAPPII is not required for an initial recruitment of YFP:RAB-A2a to membranes, but is required for its subsequent localisation dynamics during cell plate expansion (Fig. S7, compare to Fig. 4a). In conclusion, YFP:RAB-A2a and

TRS120:mCherry colocalize at the cell plate throughout cytokinesis and YFP:RAB-A2a localisation dynamics depend on TRAPPII function.

An analysis of dominant negative versus constitutively active RAB-A2a variants provide genetic evidence that TRAPPII is a RAB-A2a GEF

The above observations support a scenario in which RAB-A2a requires TRAPPII for its proper localisation at the cell plate. As TRAPPII is a known Rab GEF in yeast and metazoans (Morozova et al., 2006; Riedel et al., 2018), we hypothesised that TRAPPII may act as a GEF for RAB-A2a in Arabidopsis and therefore be required for its proper localisation during cytokinesis. To test this, we visualized dominant negative and constiutively active RAB-A2a variant localisation, expressed from the native promotor, in wild-type versus *trappii* mutant backgrounds. In the wild-type background, YFP:A2a-DN was recruited to the cell plate and at least partially relocalized to its leading edges at the end of cytokinesis (Fig. 4e; Fig. S7). This is inconsistent with the prediction that a GDP-bound Rab should be cytosolic yet congruent with previous work showing that dominant-negative Rab GTPase mutants can retain membrane localisation, and that YFP:A2a-DN retains cell plate localisation (Asaoka et al., 2013; Chow et al., 2008). In contrast, in *trs120-4* mutants, YFP:A2a-DN was not present at the cell plate but rather labeled the cytosol or endosomal (or FM4-64 positive) compartments in the vicinity of the plate (Fig. 4f). Strikingly, in *trs33-1* mutants YFP:A2a-DN-labelled compartments formed a cloud in the vicinity of the cell plate (Fig. S6b, reminiscent of the appearance of KNOLLE-positive cytokinetic compartments in *trappii* mutants (Jaber et al., 2010; Thellmann et al., 2010; Rybak et al., 2014)). Taken together, the data correspond to a synthetic enhancement of the putatively GDP-bound YFP: A2a-DN localisation phenotype.

YFP:A2a-CA labelled wild-type cell plates in a more uniform manner than YFP:RAB-A2a (Fig. 4g, compare to Fig. 4a). YFP:A2a-CA also ectopically labeled the plasma membrane in wild-type mitotic cells (Fig. 4g); the ratio of cell plate to plasma membrane signal intensity was roughly 1.0 (Fig. 4d). In *trappii* mutants, cell plate labeling was stronger and ectopic plasma membrane localisation significantly weaker (Fig. 4d, Fig. 4h). This was also seen in *trs33-1* mutants (Fig. S6c,d; Fig. S7d) and corresponds to a partial suppression of the GTP-bound YFP:A2a-CA localisation phenotype. To interpret these observations, one should bear in mind that GDP/GTP-bound mutants are not absolute but on a gradient and that TRAPPII is not the sole component required for RAB-A2a membrane association (as shown in Fig. 4b and 4c above). One would thus predict that a GEF knockout would increase the GDP-bound and decrease the GTP-bound Rab

pools and, accordingly, enhance or (at least partially) suppress the respective phenotypes. YFP:A2a-CA is indeed more properly localized at the cell plate in TRAPPII mutants, which amounts to partial suppression. In conclusion, our data show that *trappii* mutations enhance the GDP-bound YFP:A2a-DN phenotype and partially suppress the putative GTP-bound YFP:A2a-CA phenotype, which provides very compelling genetic evidence that TRAPPII functions upstream of RAB-A2a.

In a reciprocal approach, we examined the impact of YFP:A2a-CA overexpression on the seedling lethal phenotype of a *trappii* null mutant. YFP:A2a-CA was expressed from the constitutive P35S promotor and crossed into *club-2*, a null, seedling-lethal allele, and expression levels were tested by Western blot analysis. We found that YFP:A2a-CA expression partially suppressed the seedling lethality of *club-2* mutants, in a manner similar to that previously reported for a constitutively active variant of RAB-A1c (Qi et al., 2011; Qi & Zheng, 2011). 12 days after germination, *club-2* mutants expressing YFP:A2a-CA or YFP:A1c-CA had significantly longer primary roots than the *club-2* mutants alone (P < 0.004; Fig. S8). We noted that these rescued mutants developed true leaves and survived for 7-10 days longer than *club-2.* Together with the enhancement or suppression of YFP:A2a-DN or -CA localisation phenotypes in *trappii* mutants, this genetic suppression of the *trappii* phenotype by a constitutively active RAB-A2a variant provides strong evidence that TRAPPII acts upstream of RAB-A2a. These lines of evidence, along with the known roles of TRAPPII in yeast and metazoans, strongly support a scenario in which TRAPPII is a GEF for RAB-A2a in Arabidopsis.

Discussion

TRAPP complexes are known regulators of membrane traffic in both yeast and metazoans, with two complexes (TRAPPII and TRAPPIII) well characterized in yeast and metazoans (Thomas et al., 2018; Riedel et al., 2018). In both yeast and metazoans, TRAPP complexes act as GEFs for Rab GTPases. In *Arabidopsis*, genetic evidence has previously shown that TRAPPII is essential for cytokinesis and cell polarity in plants, supporting a role for this complex in trafficking at and from the TGN/EE (Jaber et al., 2010; Thellmann et al., 2010; Qi et al., 2011; Ravikumar et al., 2018). Here, we show that homologues of all known yeast and metazoan TRAPP subunits are present in the *Arabidopsis* proteome. Based on these proteomic and additional binary interaction data, we propose a dimerized model for Arabidopsis TRAPPII structure, with plant-specific domains of TRAPPII subunits at the centre of the complex. We provide five lines of

evidence that TRAPPII acts as an upstream regulator of RAB-A2a and propose that TRAPPII is likely a GEF for RAB-A2a. First, TRAPPII components preferentially interacted with a GDP-bound mutant of RAB-A2a compared to wild-type or GTP-bound RAB-A2a. Second, YFP:RAB-A2a was shown to depend on an intact TRAPPII complex for its proper localisation to the leading edges of expanding cell plates. Third, the aberrant localisation of a dominant negative variant of YFP:RAB-A2a was enhanced in a *trappii* mutant background. Fourth, the localisation phenotype of a constitutively active variant of YFP:RAB-A2a was partially suppressed by a *trappii* mutant background. Finally, the seedling lethal *trappii* phenotype was partially suppressed by a constitutively active variant of YFP:RAB-A2a. Taken together, these independent lines of investigation provide strong evidence for a regulatory function of TRAPPII upstream of RAB-A2a, likely as a Rab GEF.

Our observations support the hypothesis that *Arabidopsis* has multiple TRAPP complexes with distinctive modes of interaction with *Arabidopsis* Rab GTPases (Fig. 5). They also demonstrate the strength of the differential IP-MS strategy, which is based on the observation that cognate GEFs preferentially bind GDP-bound Rab GTPases whereas downstream effectors have a greater affinity for GTP-bound Rab GTPases (Lai et al., 1993; Day et al., 1998; Goh et al., 2007; Preuss et al., 2006; Camacho et al., 2009). All 13 Arabidopsis TRAPP subunits co-purified with CLUB/AtTRS130 and wild-type RAB-A2a in our IP-MS analyses. Binding to wild-type TRAPP subunits or Rab GTPases, however, does not provide information regarding complex composition. In contrast, such information was provided by our differential IP-MS strategy. Indeed, the 13 *Arabidopsis* TRAPP subunits could be clearly divided into two distinct groups based on their relative interaction with the GDP or GTP-bound forms of RAB-A2a. The first group consisted of *Arabidopsis* homologues of all metazoan TRAPPII subunits, including a previously unrecognized AtTRS20/TCA17/TRAPPC2(L) homologue and AtTRS33. The yeast homologue of AtTRS33 is a component of both TRAPPII and possibly TRAPPIV (Lipatova et al., 2016). The synergistic genetic interaction we report between *trs33* and a *trappii*-specific allele leads to the conclusion that AtTRS33 is a likely component of TRAPPII in Arabidopsis, in line with both yeast and metazoans. This is also supported by our yeast two-hybrid analyses, which indicate a binary interaction between AtTCA17/TRAPPC2L and AtTRS33.

In contrast to TRAPPII subunits, which were defined as preferentially binding to the GDP-bound Rab-A2a variant, a second set of *Arabidopsis* TRAPP subunits was distinguished by their failure to interact with the GDP-bound form of RAB-A2a. This set of subunits may therefore interact with RAB-A2a as effectors rather than as a GEF. Among these was

AtTRS65/TRAPPC13, which is a component of yeast TRAPPII but of metazoan TRAPPIII (Kim et al., 2016; Riedel et al., 2008). Two additional subunits in this class were characteristic of metazoan TRAPPIII but are not present in yeast TRAPPIII and have not previously been recognized in plant genomes. These subunits preferentially bound the vacuolar RAB-G3f. In conclusion, our differential IP-MS strategy, which uses different Rab GTPase clades and variants as baits, points to the *in vivo* existence of a plant complex differing from yeast but closely resembling metazoan TRAPPIII in terms of subunit composition. The differential IP-MS strategy may thereby be enabling us to distinguish between different complexes involved in biosynthetic versus degradative trafficking routes.

To characterize the Arabidopsis TRAPPII complex, we performed an extensive investigation of binary interactions using yeast two-hybrid analyses. Previous work in yeast and metazoans has proposed structures for TRAPPII and TRAPPIII, including a crystal structure for a core TRAPP subcomplex (Kim et al., 2006; Yip et al., 2010; Tan et al., 2013). In the case of TRAPPII, a dimerized structure in both yeast and metazoans is supported by electron microscopy and binary interaction assays (Yip et al., 2010; Taussig et al., 2013). Our results constitute an investigation of TRAPPII structure in plants and align with the previously proposed crystal structure of core-TRAPP subunits in yeast (Kim et al., 2006). Our observation that AtTCA17 is a binary interactor of CLUB/AtTRS130 and AtTRS33 supports reports in yeast that TCA17 is a component of TRAPPII (Scrivens et al., 2009; Montpetit & Conibear, 2009; Wang et al., 2014).

In 2013, Taussig and colleagues proposed four distinct possible dimerized structures for yeast TRAPPII, favouring two models with subunits Trs130 and Trs65 at the centre of the TRAPPII dimer (Taussig et al., 2013). Our yeast two-hybrid analyses are consistent with reported interactions between Tca17/TRAPPC2L and Trs130/TRAPPC10 (Choi et al., 2011; Milev et al., 2018). Moreover, binary interactions between AtTRS120 truncations and between AtTRS120 and CLUB/AtTRS130 truncations that are indicated by our yeast two-hybrid analyses support a model for Arabidopsis TRAPPII structure with dimerized TRS120 at the centre of the complex (Figure 1). The arrangement of subunits proposed in our model is also supported by IP-MS analyses, in which the highest-ranking interactors of CLUB/AtTRS130 amongst TRAPP subunits are predicted to be adjacent to or one subunit removed from CLUB/AtTRS130 in our model. Such a model was considered but subsequently excluded by Taussig and colleagues (2013) for yeast TRAPPII on the basis that Trs120 interacts with Trs20 and Trs33 but not with itself. However, we failed to detect binary interactions between truncated versions of AtTRS120 and full-length AtTRS33 in our yeast two-hybrid analyses; this interaction is key to the

two dimerized structure models favoured by Taussig et al., 2013. Nonetheless, in their original model Yip et al. (2010) point out that yeast Trs120 and Trs130 are involved in constructing the dimer interface, which is consistent with our model.

The major discrepancy between our Arabidopsis dimerized model and yeast models is the role for Trs65/Kre11 in either forming or stabilizing the TRAPPII dimer in yeast (Yip et al., 2010; Taussig et al., 2013). In this study, we have identified a hitherto unannotated Arabidopsis AtTRS65/TRAPPC13 homologue and attributed this not to TRAPPII as in yeast but to TRAPPIII as in metazoans. This is on the basis of clustering of AtTRS65 with TRAPPIII-specific subunits in a YFP: RAB-G3f IP-MS and lack of binding to YFP: A2a-DN (and hence negative values in the pairwise comparisons A2a DN/WT and A2a DN/CA). In these respects, AtTRS65 is identical to Arabidopsis homologues of the metazoan TRAPPIII subunits TRAPPC8, TRAPPC11, TRAPPC12. The attribution of AtTRS65 to TRAPPIII poses the question as to how the proposed Arabidopsis TRAPPII dimer is formed or stabilized. Tokarev et al., 2009, report that yeast TRAPP II complex assembly requires either Trs33 or Trs65, and we show here that an Arabidopsis TRAPPII-specific subunit interacts genetically with *TRS33*. Whether TRS33 can replace TRS65 function in Arabidopsis TRAPPII is unclear. The Arabidopsis TRAPPII interactome is vast and unexplored and could contain a plant-specific TRS65 orthologue that helps build or stabilize the TRAPPII complex. Our analyses identified strong interactions between regions of AtTRS120 and CLUB/AtTRS130 that are poorly conserved with respect to their yeast and metazoan homologues. These plant-specific TRAPPII regions appear to form the core of a dimerized Arabidopsis TRAPPII. This feature raises interesting possibilities as to whether such plant-specific regions of TRAPPII are sites of TRAPPII interactions with plant-specific components capable of replacing TRS65 and whether they function to support plant-specific requirements of endomembrane traffic.

The Arabidopsis TRAPPII complex has been shown to play a pivotal role in a variety of sorting decisions implicating different steps in the secretory pathway (Steiner et al., 2016a; Ravikumar et al., 2018). One of the first steps in the secretory pathway is entry into the Golgi apparatus from the endoplasmic reticulum. In yeast, this step is thought to be mediated by TRAPPIII acting as a GEF to activate Ypt1 at the cis-Golgi (Thomas et al., 2018; Fig. 5a). Metazoan TRAPPII has been shown to possess GEF activity for both Rab-1 (orthologues of Ypt1) and Rab11 (orthologues of Ypt31/32; Riedel et al., 2018; Fig. 5b). Plant Ypt1/Rab-1 orthologues are Rab-D GTPases, which localize to the Golgi and mediate ER-Golgi traffic (Pinherio et al., 2009). It is interesting that a Rab-D member

was found to co-purify with a TRAPPII specific subunit in this study. A previous study has shown that a constitutively active Rab-D variant fails to suppress the *trappii* phenotype (Qi and Zheng, 2011). A possible interpretation of these two apparently contradictory findings is that Rab-D might act upstream of TRAPPII in a -D/TRAPPII/Rab-A cascade that mediates entry into and exit from the Golgi (Fig. 5c). Thus, Rab-D may recruit TRAPPII as an effector and possibly co-ordinate its putative GEF activity towards downstream Rab GTPases. Following entry into the Golgi, the next steps in biosynthetic trafficking routes are passage through the Golgi, Golgi exit, sorting at the TGN/EE and exocytosis. These steps may be mediated by a sequence of events implicating Rab-B (intra-Golgi traffic), Rab-A (TGN/EE, post-Golgi traffic), and Rab-E (Golgi to PM). In this context, it is interesting that *trappii* mutants have a disrupted Golgi morphology, and are impacted in all aspects of TGN/EE function, including exocytosis (Ravikumar et al., 2018). Conversely, Rab-F or Rab-G clades were not robustly identified in the CLUB/AtTRS130 interactome in this study and *trappii* mutants are not impaired in vacuolar trafficking (Ravikumar et al., 2018). Thus, the identification of four Rab clades implicated in biosynthetic trafficking routes and the absence of late endosomal or vacuolar Rab GTPases in the CLUB/AtTRS130 interactome may turn out to be of true biological relevance.

Many questions remain regarding TRAPP complex modularity and function in plants. Here we have provided *in vivo* biochemical and genetic evidence that Arabidopsis TRAPPII acts upstream of a Rab-A2 GTPase, highlighting TRAPPII as a likely Rab GEF in Arabidopsis. Previous reports (Qi et al., 2011; Qi and Zheng, 2011) have functionally linked TRAPPII with a Rab-A1 GTPase. The A1 and A2 Rab clades have been shown to act in distinct steps of subcellular trafficking (Choi et al., 2013). This and the observation that constitutively active variants of distinct Rab-A GTPases can only partially rescue a *trappii* mutant suggests that TRAPPII may activate multiple Rab-As. However, whether or not TRAPPII may act as a universal GEF for all six Arabidopsis Rab-A clades remains to be determined. Given the striking expansion of the Rab-A clade in Arabidopsis compared to Rab11 in metazoans, it is also tempting to speculate as to the existence of as yet unidentified GEFs other than TRAPPII that might activate Rab-As in Arabidopsis. Indeed, as well as TRAPPII, Riedel and colleagues identify Parcas as a GEF for Rab11 in Drosophila (Riedel et al., 2018). The Arabidopsis genome, however, does not appear to encode Parcas homologues. Another open question is the extent to which Rab GEFs influence the membrane association of Rab GTPases. It is generally accepted that GEFs are central in determining Rab spatial distribution; accordingly, mis-targeting of Rab GEFs has been shown to mis-localise their cognate Rab GTPases (Blümer et al., 2013).

However, the classic view that GDP-bound Rab GTPases are cytosolic is contested by the observations presented in this study, in Chow et al. (2008) and in Asaoka et al. (2013). Furthermore, Rab-GTPases can remain membrane associated in the absence of their known GEF (Cabrera & Ungermann, 2013), suggesting that additional factors may promote Rab membrane association. In fact, Ito et al., 2018, propose a system whereby an inactive Rab is recruited to membranes by interaction with an effector that acts as a multivesicular body/late endosomal landmark and a platform for subsequent Rab activation by its cognate GEF. It is, therefore, possible that the membrane association of YFP: RAB-A2a we observe in *trappii* mutants may be due to the existence of multiple Rab-A GEFs in Arabidopsis or of additional factors that promote Rab GTPase membrane association. Whilst YFP:A2a-DN remains associated with the cell plate during cytokinesis in a wild-type background, this association is lost when YFP:A2a-DN is expressed in *trappii* mutant backgrounds. It is tempting to speculate that the loss of substantial YFP:A2a-DN membrane-association is due to the inability of this mutant variant to resist membrane extraction by a Rab GDP Dissociation Inhibitor (GDI) in the absence of its possible GEF, TRAPPII. GDIs preferentially interact with GDP-bound Rab GTPases and in yeast the Rab Ypt7 requires its cognate GEF to counteract extraction from membranes by GDI (Ueda et al., 1990; Sasaki et al., 1990; Cabrera & Ungermann., 2013). Rab GDIs remain poorly characterized in plants, and more work is required to fully understand the dynamics of plant Rab GTPase cycling.

Finally, whether the trafficking and protein sorting defects characteristic of *trappii* mutants (Rybak et al., 2014; Ravikumar et al., 2018) are due to lack of activation of one or more Rab-A GTPases in these mutants, or due to possible interactions between TRAPPII and other trafficking regulators, remains to be determined.

Enrichment of three previously unrecognised *Arabidopsis* TRAPPIII subunits in our IP-MS analyses targeted against YFP:RAB-G3f provide prima facie evidence for the existence of a second, TRAPPIII, complex (Fig. 5). This is particularly interesting given that TRAPPIII is known in both yeast and mammals to be involved in autophagy (Lamb et al., 2016; reviewed by Kim et al., 2016 & Sacher et al., 2018) and that Rab-G has been implicated in autophagy in *Arabidopsis* (Kwon et al., 2013).The role of TRAPPIII in plants and its possible connection to Rab-G GTPases are questions that merit further investigation. Another open question pertains to the possible regulation of GEF activity and specificity and whether distinct pools of TRAPPII activity exist within plant cells. In metazoans, Rab GEF activity and specificity have been shown to be influenced by post-translational modifications, association with the cytoskeleton and interaction with Rab hypervariable sequences (Thomas et al., 2019; Wang et al., 2015; Xu et al., 2018).

Previous work demonstrating interaction between Arabidopsis TRAPPII and microtubule-associated MAP65 would provide an interesting framework for the study of the regulation of TRAPPII function in Arabidopsis (Steiner et al., 2016).

Central to the function of the membrane trafficking system is the ability of individual endomembrane organelles to maintain a unique functional identity despite constant influx and export of material via vesicle exchange with other compartments. An example is the maintenance of plasma membrane identity in the face of influx of *trans*-Golgi membrane from the secretory pathway. Another important process is the maturation of one membrane compartment into another over time; examples here include early- to late-endosome, *cis*- to *trans*-Golgi and cell plate to cross wall transitions (Bottanelli et al., 2012; Cui et al., 2014; Rybak et al., 2014). In Arabidopsis, TRAPPII has been shown to be required for the maturation of the cell plate from a juvenile compartment into a cross wall (Rybak et al., 2014). Organised changes in membrane identity over time have been attributed to Rab cascades, in which Rab-GEF interactions play a central role (Ravikumar et al., 2017). The observation in this study that a TRAPPII-specific component uncovered TRAPPIII-specific subunits may appear surprising, but it is to be noted that interactions between distinct tethering complexes have been shown to orchestrate a sequence of events during cell plate maturation in Arabidopsis (Rybak et al., 2014). By analogy, it is tempting to speculate that the presence of TRAPPIII subunits at low abundance in TRAPPII IP-MS samples might reflect a coordination between biosynthetic and degradative trafficking routes. The differential IP-MS strategy, elaborated in this study as being able to discriminate between putative Rab GEFs versus Rab effectors, can be reiterated with different Rab GTPases to assess the breadth of TRAPP GEF specifity in plants. Our characterization of the TRAPPII complex and its identification as a putative Rab GEF in this study opens up the future possibility of reconstituting the complex and assessing its GEF activity via direct *in vitro* assays. Understanding the nature of GEF-Rab interactions will be crucial to understanding the steady-state operation of plant membrane traffic and the mechanisms that alter trafficking pathways in response to developmental or physiological signals.

EXPERIMENTAL PROCEDURES

Lines and growth conditions

All the lines used in this study are listed in Table S1 Seedling-lethal mutants were propagated as hetero- or hemi-zygotes. Insertion lines were selected via the TAIR and NASC web sites (Swarbreck et al., 2008). Plants were grown in the greenhouse under controlled temperature conditions and with supplemental light, or under controlled growth chamber conditions (16/8 hr photoperiod at 250 µmol m^{-2}s^{-1}). Seedlings were surface sterilized, stratified at 4°C for two days and plated on ½ MS medium supplemented with 1% sucrose and B5 Vitamins (Sigma; https://www.sigmaaldrich.com). Plates were incubated in the light for all lines but *trs33-1*, which were grown in the dark. The root tips or hypocotyls of five-day old plate grown seedlings were used for light, confocal and electron microscopy.

Co-immunoprecipitation

For TRAPPII baits, co-immunoprecipitation experiments were carried out on three grams of tissue using GFP-trap beads (Chromotek), as described (Rybak et al., 2014). In pilot experiments, we tested inflorescences, seedlings and leaves; inflorescences were then used for replicate experiments as we identified the largest complement of TRAPP subunits in this tissue type. NanoflowLc-MS/MS was performed by coupling an EksigentnanoLC-Ultra 1D+ (Eksigent, Dublin, CA) to a Velos-LTQ-Orbitrap (Thermo Scientific, Bremen, Germany; see Supplemental methods).

For RAB-A2a baits, co-IP experiments were carried out by isolating total microsomes from Arabidopsis roots expressing YFP:RAB-A2a, YFP: RAB-A2a[Q71L] and YFP: RAB-A2a[S26N] (Chow et al., 2008), YFP: RAB-G3f (Geldner et al., 2009) and no transgene. Plants were grown in 20mL 0.3x Murashige and Skoog medium (Sigma-Aldrich, Poole, UK) with 1% sucrose and 0.05% MES, pH5.7 shaking at 60rpm (16h day: 8h night cycle, 21°C) for 14 days. 5µM NAA (naphthyl acetic acid) was then added and plants allowed to continue growth for 3 days. Microsomes were isolated from root tissue for immunoprecipitation with anti-GFP µMACS magnetic microbeads (Miltenyi Biotec, Woking, UK), as described in the supplemental methods. In-gel trypsin digest and mass spectrometry were performed by the Central Proteomic Facility, University of Oxford (www.proteomics.ox.ac.uk) and the proteome quantified as described in the supplemental methods. Co-immunoprecipitated proteins were quantified from 3

independent experiments (with three biological replicates for the Rab baits and six biological replicates for the negative controls) and any protein also present in negative controls (no-transgene Columbia samples) was excluded from the analysis.

LC/MS analysis is described in detail in the supplemental methods. Briefly, protein identifications were filtered to 1% protein false-discovery rate. We used a cutoff of at least two unique peptides for TRAPP subunits for identification. For Rab GTPases, however, the high degree of homology between paralogues (especially in the vastly expanded Rab-A clade) impedes the identification of unique peptides and we took razor peptides common to subfamilies into account as well, filtering for at least four peptides (unique + shared/razor). In downstream analysis, we used intensity-based absolute quantification (iBAQ) (Schwanhaeusser et al. 2011), which represents an estimate of the absolute concentration of a given protein. Before statistical analysis, iBAQ intensities were normalized according the iBAQ intensity of the bait protein in the respective co-immunoprecipitation (IP). Normalized iBAQ intensities were used to calculate protein ratios between groups as well as to compare the relative concentration of different TRAPP subunits and RAB GTPases within one group. Log2 ratios, computed as the average intensity in the experiment compared to the average intensity in the negative control, were considered high if larger than 8, and intermediate if in the 5-8 range. In the tables, all detected TRAPP subunits and Rab GTPases were ranked according to their ratio between the experiment and negative control. The number of proteins detected in IP-MS experiments is tabulated in Table S2. The two-sided Student t-test was used to evaluate the significance of mean differences in all comparisons. A P-value cutoff of 0.02 was used to determine significance.

Confocal microscopy.

Confocal microscopes used for imaging were an Olympus (www.olympus-ims.com) Fluoview 1000 confocal laser scanning microscope (CSLM) and a Leica (www.leica-microsystems.com) SP8 Hyvolution CSLM. Cell cycle stage was determined via time laspes in live imaging. Images taken with the Leica SP8 microscope were deconvolved using the built-in Huygens Scientific deconvolution software (www.leicamicro-systems.com) operated in both 2D and 3D. Cell cycle stages (depicted as described by Smertenko et al., 2017) were determined via TRS120-GFP and YFP:RAB-A2a localisation dynamics, taking into account how membrane markers follow phragmoplast microtubule dynamics (Steiner et al., 2016a). As TRAPPII affects both phragmoplast microtubule dynamics (Steiner et al., 2016a) and YFP:RAB-A2a localisation, we also

relied on FM4-64 to image cell plates in *trappii* mutants. As we only monitor the cell plate, cytokinesis is broadly split into cell plate biogenesis (encompassing disc and ring phragmoplast stages), cell plate expansion (encompassing more specifically the ring phragmoplast stage; telophase) and cell plate maturation (following cell plate anchoring, encompasses the discontinuous phragmoplast stage and post-telophase; Smertenko et al., 2017).

Histological sections and Light Microscopy.

For an analysis of embryogenesis in double mutants, we dissected the mature siliques of plants segregating the *trapp* T-DNA insertions (as verified by PCR analysis). Embryos were harvested, fixed, infiltrated, embedded and imaged as described (Matthes and Torres-Ruiz, 2016).

Statistical analysis and image processing

False discovery rates, determined with the standard two-tailed t-test, were set at a cutoff of 1%. Images were processed with Adobe photoshop (www.adobe.com) and GIMP (https://www.gimp.org), analyzed with Image J (https://imagej.nih.gov), and assembled with Inkscape (https://inkscape.org).

Yeast Two-Hybrid (Y2H).

Y2H screens were performed as described (Dreze et al., 2010). TRAPPII-specific (AtTRS120 and CLUB/AtTRS130) truncations are described in Steiner et al., 2016; shared TRAPP subunits were obtained from Arabidopsis full-length cDNA clones developed by the plant genome project of RIKEN Genomic Sciences Center (Seki et al., 1998; Seki et al., 2002) or from a collection of 12,000 Arabidopsis ORFs (Wessling et al., 2014). We used the GAL4 DNA-binding domain (DB) encoding Y2H vector pDEST-pPC97, subsequently transformed into the yeast strain Y8930, as well as gene fusions to the Gal4 activation domain (AD) in the yeast strain Y8800 (Altmann et al., 2018). The constructs were screened by yeast mating in quadruplicate pair-wise tests. Screening was done as a binary mini-pool screen, *i.e.* each DB-ORF was screened against pools of 188 AD-ORFs. Interactions were assayed by growth on selective plates using the *HIS3* reporter, and using 1mM 3-Amino-1,2,4-triazole (3-AT) to suppress background growth.

This primary screen was carried out once and interaction candidates were identified by Sanger sequencing. All candidate interactions were verified by pairwise one-on-one mating in four independent experiments. Only pairs scoring positives in all four assays were considered as *bona fide* interaction partners. The use of low-copy plasmids, weak promotors, the counter-selectable marker cyh2^S on the AD-Y plasmid as well as semi-quantitative scoring of quadruplicate tests has been shown to reliably eliminate experimental artifacts and hence false-positives.

ACCESSION NUMBERS

Sequence data from this article can be found in the Arabidopsis Genome Initiative database under the accession numbers listed in Table I and Table II. All data that support the conclusions of this study are available upon request. The authors responsible for distribution of materials in accordance with the policy described in the Instructions for Authors are: Farhah Assaad (Farhah@wzw.tum.de); Liam Elliott (liam.elliott@plants.ox.ac.uk).

DATA DEPOSITION

Mass spectrometry data have been deposited at the ProteomeXchange Consortium (http://proteomecentral.proteomexchange.org) via the PRIDE partner repository with the dataset identifier PXD013016.

FUNDING

AUTHOR CONTRIBUTIONS

M.K., R.R., B.A, C.W., N.K., A.S., L.E. and F.F.A. designed and performed experiments, analysed, quantified, interpreted and presented data. M. Altmann designed and performed yeast two-hybrid experiments. M. Abele elucidated complex topology based on binary interaction data. M.K., K.R., S.K., B.K., C.L., C.M. and I.M. generated and/or analysed mass spectrometry datasets. X.Q, and H.Z. contributed genetic suppression data. R.R., M.Altmann, M.Abele and X.Q assembled figure panels. F.F.A., P. F-B. and I.M. acquired funding and supervised experiments. I.M drafted sections of the manuscript. F.F.A. and L.E. wrote and revised the manuscript with input from all co-authors.

SUPPLEMENTAL INFORMATION

Figure S1. Volcano plot showing all co-purified proteins in a CLUB-GFP immunoprecipitate. *Related to Tables I and II.*

Figure S2. Reciprocal pair-wise Y2H tests between TRAPP subunits. *Related to Figure 1.*

Figure S3. Incidence of double mutant *club trs33* embryo phenotypes. *Related to Figure 2.*

Figure S4. Peptide coverage for RAB-A2a in IP-MS with CLUB as bait. *Related to Table II.*

Figure S5. Volcano plot showing all co-purified proteins in a YFP: RABA2a immunoprecipitate. *Related to Table III*

Figure S6. Sorting of YFP: RAB-A2a GDP or GTP bound variants in *trs33-1* root tips. *Related to Figure 4 and Figure S7.*

Figure S7. The behavior of YFP: RAB-A2a, -DN and -CA in wild-type versus *trapp* root tips. *Related to Figure 4 and Figure S6.*

Figure S8. Genetic suppression of *trappii* seedling lethal phenotype by YFP:A2a-CA. *Related to Figure 4.*

Table S1. Mutant lines used in this study.
Table S2. Number of proteins identified in IP-MS experiments.

Supplemental Experimental Procedures

Supplemental References
References

- Ahn, C.S., Han, J.-A., Pai, H.-S. (2013). Characterization of in vivo functions of Nicotiana benthamiana RabE1. Planta 23: 161–172.
- Altmann, M., Altmann, S., Falter, C., Falter-Braun, P. (2018). High-Quality Yeast-2-Hybrid Interaction Network Mapping. Curr Protoc Plant Biol 3, e20067.
- Asaoka, R., Uemura, T., Ito, J., Fujimoto, M., Ito, E., Ueda, T., Nakano, A. (2013). Arabidopsis RABA1 GTPases are involved in transport between the trans-Golgi network and the plasma membrane, and are required for salinity stress tolerance. Plant J. 73, 240–249.
- Assaad, F.F., Mayer, U., Wanner, G., Jürgens, G. (1996). The KEULE gene is involved in cytokinesis in Arabidopsis. Mol Gen Genet: 253, 267–277.
- Barr, F.A. (2013). Rab GTPases and membrane identity: Causal or inconsequential? J Cell Biol 202: 191–199.
- Bassik, M.C., Kampmann, M., Lebbink, R.J., Wang, S., Hein, M.Y., Poser, I., Weibezahn, J., Horlbeck, M.A., Chen, S., Mann, M., Hyman, A.A., Leproust, E.M., McManus, M.T., Weissman, J.S. (2013). A systematic mammalian genetic interaction map reveals pathways underlying ricin susceptibility. Cell: 152, 909–922.
- Blümer, J., Rey, J., Dehmelt, L., Mazel, T., Wu, Y.-W., Bastiaens, P., Goody, R.S., Itzen, A. (2013). RabGEFs are a major determinant for specific Rab membrane targeting. J Cell Biol 200, 287–300.
- Bottanelli, F., Gershlick, D.C., Denecke, J. (2012). Evidence for sequential action of Rab5 and Rab7 GTPases in prevacuolar organelle partitioning. Traffic 13: 338–354.
- Cabrera, M., Ungermann, C. (2013). Guanine Nucleotide Exchange Factors (GEFs) Have a Critical but Not Exclusive Role in Organelle Localization of Rab GTPases. J Biol Chem 288, 28704–28712.
- Camacho, L., Smertenko, A.P., Pérez-Gómez, J., Hussey, P.J., Moore, I. (2009). Arabidopsis Rab-E GTPases exhibit a novel interaction with a plasma-membrane phosphatidylinositol-4-phosphate 5-kinase. Journal of Cell Science 122: 4383–4392.
- Choi, C., Davey, M., Schluter, C., Pandher, P., Fang, Y., Foster, L.J., Conibear, E. (2011). Organization and Assembly of the TRAPPII Complex. Traffic 12, 715–725.
- Choi, S., Tamaki, T., Ebine, K., Uemura, T., Ueda, T., Nakano, A. (2013). RABA members act in distinct steps of subcellular trafficking of the FLAGELLIN SENSING2 receptor. Plant Cell 25, 1174–1187.

- Chow, C.-M., Neto, H., Foucart, C., Moore, I. (2008). Rab-A2 and Rab-A3 GTPases Define a trans-Golgi Endosomal Membrane Domain in Arabidopsis That Contributes Substantially to the Cell Plate. Plant Cell 20: 101–123.

- Costes, S.V., Daelemans, D., Cho, E.H., Dobbin, Z., Pavlakis, G., Lockett, S. (2004). Automatic and Quantitative Measurement of Protein-Protein Colocalization in Live Cells. Biophys J 86: 3993–4003.

- Cui, Y., Zhao, Q., Gao, C., Ding, Y., Zeng, Y., Ueda, T., Nakano, A., Jiang, L. (2014). Activation of the Rab7 GTPase by the MON1-CCZ1 Complex Is Essential for PVC-to-Vacuole Trafficking and Plant Growth in Arabidopsis. Plant Cell 26: 2080–2097.

- Day, G.-J., Mosteller, R.D., Broek, D. (1998). Distinct Subclasses of Small GTPases Interact with Guanine Nucleotide Exchange Factors in a Similar Manner. Mol Cell Biol 18: 7444–7454

- Der, C.J., Finkel, T., Cooper, G.M. (1986). Biological and biochemical properties of human rasH genes mutated at codon 61. Cell 44: 167–176.

- Dettmer, J., Hong-Hermesdorf, A., Stierhof, Y.-D., Schumacher, K. (2006). Vacuolar H+-ATPase Activity Is Required for Endocytic and Secretory Trafficking in Arabidopsis. Plant Cell 18: 715–730.

- Drakakaki, G., van de Ven, W., Pan, S., Miao, Y., Wang, J., Keinath, N.F., Weatherly, B., Jiang, L., Schumacher, K., Hicks, G., and Raikhel, N. (2012). Isolation and proteomic analysis of the SYP61 compartment reveal its role in exocytic trafficking in Arabidopsis. Cell Res 22, 413-424.

- Dreze, M., Monachello, D., Lurin, C., Cusick, M., Hill, D., Vidal, M., Falter-Braun, P. (2010a). High-Quality Binary Interactome Mapping. Methods in enzymology 470: 281–315.

- Dreze, M., Monachello, D., Lurin, C., Cusick, M.E., Hill, D.E., Vidal, M., Braun, P. (2010b). High-Quality Binary Interactome Mapping, in: Methods in Enzymology. Elsevier, pp. 281–315.

- Fukuda, M., Wen, L., Satoh-Cruz, M., Kawagoe, Y., Nagamura, Y., Okita, T.W., Washida, H., Sugino, A., Ishino, S., Ishino, Y., Ogawa, M., Sunada, M., Ueda, T., Kumamaru, T. (2013). A Guanine Nucleotide Exchange Factor for Rab5 Proteins Is Essential for Intracellular Transport of the Proglutelin from the Golgi Apparatus to the Protein Storage Vacuole in Rice Endosperm. Plant Physiol 162: 663–674.

- Geldner, N., Dénervaud-Tendon, V., Hyman, D.L., Mayer, U., Stierhof, Y.-D., Chory, J. (2009). Rapid, combinatorial analysis of membrane compartments in intact plants with a multicolor marker set. Plant J. 59: 169–178.

- Goh, T., Uchida, W., Arakawa, S., Ito, E., Dainobu, T., Ebine, K., Takeuchi, M., Sato, K., Ueda, T., Nakano, A. (2007). VPS9a, the common activator for two distinct types of Rab5 GTPases, is essential for the development of Arabidopsis thaliana. Plant Cell 19: 3504–3515.

- Guarente, L., 1993. Synthetic enhancement in gene interaction: a genetic tool come of age. Trends Genet: 9, 362–366.

- Ito, E., Ebine, K., Choi, S., Ichinose, S., Uemura, T., Nakano, A., Ueda, T., 2018. Integration of two RAB5 groups during endosomal transport in plants. eLife: 7, e34064.

- Jaber, E., Thiele, K., Kindzierski, V., Loderer, C., Rybak, K., Jürgens, G., Mayer, U., Söllner, R., Wanner, G., Assaad, F.F. (2010). A putative TRAPPII tethering factor is required for cell plate assembly during cytokinesis in Arabidopsis. New Phytol. 187: 751–763.

- Jia, P.-F., Xue, Y., Li, H.-J., Yang, W.-C. (2018) Golgi-localized LOT regulates trans-Golgi network biogenesis and pollen tube growth. PNAS 115: 12307–12312.

- Kim, J.J., Lipatova, Z., Segev, N. (2016). TRAPP Complexes in Secretion and Autophagy. Front Cell Dev Biol 4, 20.

- Kim, Y.-G., Raunser, S., Munger, C., Wagner, J., Song, Y.-L., Cygler, M., Walz, T., Oh, B.-H., Sacher, M. (2006). The architecture of the multisubunit TRAPP I complex suggests a model for vesicle tethering. Cell 127: 817–830.

- Koumandou, V.L., Dacks, J.B., Coulson, R.M., Field, M.C. (2007). Control systems for membrane fusion in the ancestral eukaryote; evolution of tethering complexes and SM proteins. BMC Evolutionary Biology 7, 29.

- Kwon, S.I., Cho, H.J., Kim, S.R., Park, O.K. (2013). The Rab GTPase RabG3b Positively Regulates Autophagy and Immunity-Associated Hypersensitive Cell Death in Arabidopsis. Plant Physiol: 161, 1722–1736.

- Lai, C.C., Boguski, M., Broek, D., Powers, S. (1993). Influence of guanine nucleotides on complex formation between Ras and CDC25 proteins. Mol Cell Biol 13: 1345–1352.

- Lamb, C.A., Nühlen, S., Judith, D., Frith, D., Snijders, A.P., Behrends, C., Tooze, S.A. (2016). TBC1D14 regulates autophagy via the TRAPP complex and ATG9 traffic. EMBO J: 35, 281–301.

- Lipatova, Z., Majumdar, U., Segev, N. (2016). Trs33-Containing TRAPP IV: A Novel Autophagy-Specific Ypt1 GEF. Genetics 204: 1117–1128.

- Luo, Y., Scholl, S., Doering, A., Zhang, Y., Irani, N.G., Di Rubbo, S., Neumetzler, L., Krishnamoorthy, P., Van Houtte, I., Mylle, E., Bischoff, V., Vernhettes, S., Winne, J., Friml, J., Stierhof, Y.-D., Schumacher, K., Persson, S., Russinova, E. (2015) V-ATPase activity in the TGN/EE is required for exocytosis and recycling in *Arabidopsis*. Nature Plants 1: 15094.

- Matthes, M., Torres-Ruiz, R.A. (2016). Boronic acid treatment phenocopies monopteros by affecting PIN1 membrane stability and polar auxin transport in Arabidopsis thaliana embryos. Development 143: 4053–4062.

- Mayers, J.R., Hu, T., Wang, C., Cárdenas, J.J., Tan, Y., Pan, J., Bednarek, S.Y. (2017) SCD1 and SCD2 Form a Complex That Functions with the Exocyst and RabE1 in Exocytosis and Cytokinesis. The Plant Cell 29: 2610–2625.

- Milev, M.P., Graziano, C., Karall, D., Kuper, W.F.E., Al-Deri, N., Cordelli, D.M., Haack, T.B., Danhauser, K., Iuso, A., Palombo, F., Pippucci, T., Prokisch, H., Saint-Dic, D., Seri, M., Stanga, D., Cenacchi, G., Gassen, K.L.I. van, Zschocke, J., Fauth, C., Mayr, J.A., Sacher, M., Hasselt, P.M. van. (2018). Bi-allelic mutations in TRAPPC2L result in a neurodevelopmental disorder and have an impact on RAB11 in fibroblasts. Journal of Medical Genetics 55, 753–764.

- Montpetit, B., Conibear, E. (2009). Identification of the novel TRAPP associated protein Tca17. Traffic 10: 713–723.

- Olkkonen, V.M., Stenmark, H. (1997). Role of Rab GTPases in membrane traffic. Int. Rev. Cytol. 176: 1–85.

- Paul, P., Simm, S., Mirus, O., Scharf, K.D., Fragkostefanakis, S., and Schleiff, E. (2014). The complexity of vesicle transport factors in plants examined by orthology search. PLoS One 9, e97745.

- Pérez-Pérez, J.M., Candela, H., Micol, J.L. (2009). Understanding synergy in genetic interactions. Trends Genet. 25: 368–376.

- Pinheiro, H., Samalova, M., Geldner, N., Chory, J., Martinez, A., Moore, I. (2009). Genetic evidence that the higher plant Rab-D1 and Rab-D2 GTPases exhibit distinct but overlapping interactions in the early secretory pathway. J Cell Sci 122: 749–3758.

- Preuss, M.L., Schmitz, A.J., Thole, J.M., Bonner, H.K.S., Otegui, M.S., Nielsen, E. (2006). A role for the RabA4b effector protein PI-4Kβ1 in polarized expansion of root hair cells in Arabidopsis thaliana. J Cell Biol 172: 991–998.

- Qi, X., Kaneda, M., Chen, J., Geitmann, A., Zheng, H. (2011). A specific role for Arabidopsis TRAPPII in post-Golgi trafficking that is crucial for cytokinesis and cell polarity. Plant J. 68: 234–248.

- Qi, X., Zheng, H. (2011). Arabidopsis TRAPPII is functionally linked to Rab-A, but not Rab-D in polar protein trafficking in trans-Golgi network. Plant Signal Behav 6: 1679–1683.

- Ravikumar, R., Steiner, A., Assaad, F.F. (2017). Multisubunit tethering complexes in higher plants. Curr. Opin. Plant Biol. 40: 97–105.

- Ravikumar, R., Kalbfuß, N., Gendre, D., Steiner, A., Altmann, M., Altmann, S., Rybak, K., Edelmann, H., Stephan, F., Lampe, M., Facher, E., Wanner, G., Falter-Braun, P., Bhalerao, R.P., Assaad, F.F. (2018). Independent yet overlapping pathways ensure the robustness and responsiveness of trans-Golgi network functions in Arabidopsis. Development 145.

- Riedel, F., Galindo, A., Muschalik, N., Munro, S. (2018). The two TRAPP complexes of metazoans have distinct roles and act on different Rab GTPases. J. Cell Biol. 217**:** 601–617.

- Rosquete, M.R., Davis, D.J., Drakakaki, G. (2018). The Plant Trans-Golgi Network: Not Just a Matter of Distinction. Plant Physiology 176, 187–198.

- Rutherford, S., Moore, I. (2002). The Arabidopsis Rab GTPase family: another enigma variation. Curr. Opin. Plant Biol. 5: 518–528.

- Rybak, K., Steiner, A., Synek, L., Klaeger, S., Kulich, I., Facher, E., Wanner, G., Kuster, B., Zarsky, V., Persson, S., Assaad, F.F**.** (2014). Plant cytokinesis is orchestrated by the sequential action of the TRAPPII and exocyst tethering complexes. Dev. Cell 29: 607–620.

- Sacher, M., Shahrzad, N., Kamel, H., Milev, M.P. (2018). TRAPPopathies: An emerging set of disorders linked to variations in the genes encoding transport protein particle (TRAPP)-associated proteins. Traffic: 20, 5–26.

- Sasaki, T., Kikuchi, A., Araki, S., Hata, Y., Isomura, M., Kuroda, S., Takai, Y. (1990). Purification and characterization from bovine brain cytosol of a protein that inhibits the dissociation of GDP from and the subsequent binding of GTP to smg p25A, a ras p21-like GTP-binding protein. J. Biol. Chem: 265, 2333–2337

- Schwanhäusser, B., Busse, D., Li, N., Dittmar, G., Schuchhardt, J., Wolf, J., Chen, W., Selbach, M., 2011. Global quantification of mammalian gene expression control. Nature: 473, 337–342.

- Scrivens, P.J., Shahrzad, N., Moores, A., Morin, A., Brunet, S., Sacher, M. (2009). TRAPPC2L is a Novel, Highly Conserved TRAPP-Interacting Protein. Traffic 10: 724–736.

- Scrivens, P.J., Noueihed, B., Shahrzad, N., Hul, S., Brunet, S., Sacher, M. (2011). C4orf41 and TTC-15 are mammalian TRAPP components with a role at an early stage in ER-to-Golgi trafficking. Mol Biol Cell: 22, 2083–2093

- Seki, M., Carninci, P., Nishiyama, Y., Hayashizaki, Y., Shinozaki, K. (1998). High-efficiency cloning of Arabidopsis full-length cDNA by biotinylated CAP trapper. Plant J: 15, 707–720.

- Seki, M., Narusaka, M., Kamiya, A., Ishida, J., Satou, M., Sakurai, T., Nakajima, M., Enju, A., Akiyama, K., Oono, Y., Muramatsu, M., Hayashizaki, Y., Kawai, J., Carninci, P., Itoh, M., Ishii, Y., Arakawa, T., Shibata, K., Shinagawa, A., Shinozaki, K. (2002). Functional annotation of a full-length Arabidopsis cDNA collection. Science 296, 141–145.

- Smertenko, A., Assaad, F., Baluška, F., Bezanilla, M., Buschmann, H., Drakakaki, G., Hauser, M.-T., Janson, M., Mineyuki, Y., Moore, I., Müller, S., Murata, T., Otegui, M.S., Panteris, E., Rasmussen, C., Schmit, A.-C., Šamaj, J., Samuels, L., Staehelin, L.A., Van Damme, D., Wasteneys, G., Žárský, V. (2017). Plant Cytokinesis: Terminology for Structures and Processes. Trends Cell Biol. 27, 885–894.

- Sohn, E.J., Kim, E.S., Zhao, M., Kim, S.J., Kim, H., Kim, Y.-W., Lee, Y.J., Hillmer, S., Sohn, U., Jiang, L., Hwang, I. (2003). Rha1, an Arabidopsis Rab5 homolog, plays a critical role in the vacuolar trafficking of soluble cargo proteins. Plant Cell 15: 1057–1070.

- Söllner, R., Glässer, G., Wanner, G., Somerville, C.R., Jürgens, G., Assaad, F.F. (2002). Cytokinesis-Defective Mutants of Arabidopsis. Plant Physiol: 129, 678–690.

- Speth, E.B., Imboden, L., Hauck, P., He, S.Y. (2009). Subcellular Localization and Functional Analysis of the Arabidopsis GTPase RabE. Plant Physiology 149: 1824–1837.

- Steiner, A., Müller, L., Rybak, K., Vodermaier, V., Facher, E., Thellmann, M., Ravikumar, R., Wanner, G., Hauser, M.-T., Assaad, F.F. (2016a). The Membrane-Associated Sec1/Munc18 KEULE is Required for Phragmoplast Microtubule Reorganization During Cytokinesis in Arabidopsis. Mol Plant 9: 528–540.

- Steiner, A., Rybak, K., Altmann, M., McFarlane, H.E., Klaeger, S., Nguyen, N., Facher, E., Ivakov, A., Wanner, G., Kuster, B., Persson, S., Braun, P., Hauser, M.-T., Assaad, F.F. (2016b). Cell cycle-regulated PLEIADE/AtMAP65-3 links membrane and microtubule dynamics during plant cytokinesis. Plant J. 88: 531–541.

- Swarbreck, D., Wilks, C., Lamesch, P., Berardini, T.Z., Garcia-Hernandez, M., Foerster, H., Li, D., Meyer, T., Muller, R., Ploetz, L., Radenbaugh, A., Singh, S., Swing, V., Tissier, C., Zhang, P., Huala, E. (2008). The Arabidopsis Information Resource (TAIR): gene structure and function annotation. Nucleic Acids Res 36: D1009–D1014.

- Tan, D., Cai, Y., Wang, J., Zhang, J., Menon, S., Chou, H.-T., Ferro-Novick, S., Reinisch, K.M., Walz, T. (2013). The EM structure of the TRAPPIII complex leads to the identification of a requirement for COPII vesicles on the macroautophagy pathway. PNAS 110: 19432–19437.

- Taussig, D., Lipatova, Z., Kim, J.J., Zhang, X., Segev, N. (2013). Trs20 is Required for TRAPP II Assembly. Traffic 14: 678–690.

- Thellmann, M., Rybak, K., Thiele, K., Wanner, G., Assaad, F.F. (2010). Tethering factors required for cytokinesis in Arabidopsis. Plant Physiol. 154: 720–732.

- Thomas, L.L., Joiner, A.M.N., Fromme, J.C. (2018). The TRAPPIII complex activates the GTPase Ypt1 (Rab1) in the secretory pathway. J Cell Biol 217, 283–298.

- Thomas, L.L., van der Vegt, S.A., Fromme, J.C. (2019). A Steric Gating Mechanism Dictates the Substrate Specificity of a Rab-GEF. Developmental Cell.

- Tisdale, E.J., Bourne, J.R., Khosravi-Far, R., Der, C.J., Balch, W.E. (1992). GTP-binding mutants of rab1 and rab2 are potent inhibitors of vesicular transport from the endoplasmic reticulum to the Golgi complex. The Journal of Cell Biology 119: 749–761

- Tokarev, A.A., Taussig, D., Sundaram, G., Lipatova, Z., Liang, Y., Mulholland, J.W., Segev, N., 2009. TRAPP II complex assembly requires Trs33 or Trs65. Traffic: 10, 1831–1844.

- Trudgian, D.C., Ridlova, G., Fischer, R., Mackeen, M.M., Ternette, N., Acuto, O., Kessler, B.M., Thomas, B. (2011). Comparative evaluation of label-free SINQ normalized spectral index quantitation in the central proteomics facilities pipeline. Proteomics 11: 2790–2797.

- Ueda, T., Kikuchi, A., Ohga, N., Yamamoto, J., Takai, Y. (1990). Purification and characterization from bovine brain cytosol of a novel regulatory protein inhibiting the dissociation of GDP from and the subsequent binding of GTP to rhoB p20, a ras p21-like GTP-binding protein. J. Biol. Chem: 265, 9373–9380.

- Ueda, T., Yamaguchi, M., Uchimiya, H., Nakano, A. (2001). Ara6, a plant-unique novel type Rab GTPase, functions in the endocytic pathway of Arabidopsis thaliana. EMBO J. 20: 4730–4741.

- Ueda, T., Uemura, T., Sato, M.H., Nakano, A. (2004). Functional differentiation of endosomes in Arabidopsis cells. The Plant Journal 40, 783–789.

- Vogel, U.S., Dixon, R.A., Schaber, M.D., Diehl, R.E., Marshall, M.S., Scolnick, E.M., Sigal, I.S., Gibbs, J.B. (1988). Cloning of bovine GAP and its interaction with oncogenic ras p21. Nature 335: 90–93.

- Wang, C., Gohlke, U., Roske, Y., Heinemann, U. (2014). Crystal structure of the yeast TRAPP-associated protein Tca17. The FEBS Journal 281: 4195–4206.

- Wang, J., Ren, J., Wu, B., Feng, S., Cai, G., Tuluc, F., Peränen, J., Guo, W. (2015). Activation of Rab8 guanine nucleotide exchange factor Rabin8 by ERK1/2 in response to EGF signaling. PNAS 112: 148–153.

- Weßling, R., Epple, P., Altmann, S., He, Y., Yang, L., Henz, S.R., McDonald, N., Wiley, K., Bader, K.C., Gläßer, C., Mukhtar, M.S., Haigis, S., Ghamsari, L., Stephens, A.E., Ecker, J.R., Vidal, M., Jones, J.D.G., Mayer, K.F.X., van Themaat, E.V.L., Weigel, D., Schulze-Lefert, P., Dangl, J.L., Panstruga, R., Braun, P. (2014). Convergent targeting of a common host protein-network by pathogen effectors from three kingdoms of life. Cell Host Microbe 16: 364–375.

- Woollard, A.A.D., Moore, I. (2008). The functions of Rab GTPases in plant membrane traffic. Curr. Opin. Plant Biol. 11: 610–619.

- Xu, J., Kozlov, G., McPherson, P.S., Gehring, K. (2018). A PH-like domain of the Rab12 guanine nucleotide exchange factor DENND3 binds actin and is required for autophagy. J. Biol. Chem 293: 4566-4574.

- Yip, C.K., Berscheminski, J., Walz, T. (2010). Molecular architecture of the TRAPPII complex and implications for vesicle tethering. Nat Struct Mol Biol 17: 1298–1304.

- Zhao, S., Li, C.M., Luo, X.M., Siu, G.K.Y., Gan, W.J., Zhang, L., Wu, W.K.K., Chan, H.C., Yu, S. (2017). Mammalian TRAPPIII Complex positively modulates the recruitment of Sec13/31 onto COPII vesicles. Sci Rep: 7, 43207

- Zhang, J., Chen, J., Wang, L., Zhao, S., Li, J., Liu, B., Li, H., Qi, X., Zheng, H., Lu, M. (2018) AtBET5 is essential for exine pattern formation and apical meristem organization in Arabidopsis. Plant Sci 274: 231–241.
- Zheng, H., Camacho, L., Wee, E., Batoko, H., Legen, J., Leaver, C.J., Malhó, R., Hussey, P.J., Moore, I. (2005). A Rab-E GTPase Mutant Acts Downstream of the Rab-D Subclass in Biosynthetic Membrane Traffic to the Plasma Membrane in Tobacco Leaf Epidermis. The Plant Cell 17: 2020–2036.
- Zou, S., Chen, Y., Liu, Yutao, Segev, N., Yu, S., Liu, Yan, Min, G., Ye, M., Zeng, Y., Zhu, X., Hong, B., Björn, L.O., Liang, Y., Li, S., Xie, Z. (2013). Trs130 participates in autophagy through GTPases Ypt31/32 in Saccharomyces cerevisiae. Traffic: 14, 233–246.

Yeast TRAPP	Metazoan TRAPP		AGI	IP-MS values and statistics CLUB/control				
Sub-unit	Complex	Sub-unit		unique peptides [a]	Sequence coverage %	rank [b]	ratio (log2) [c]	P [d] =
Trs130	II	C10	CLUB (bait; At5g54440)	125	74.2	1	15.08	0.0133
Tca17	Shared	C2L	At2g20930[A]	10	60	2	14.34	0.0002
Trs33		C6	At3g05000	10	48.6	3	13.14	0.0003
Bet3		C3	At5g54750	10	54.8	4	12.80	0.0003
Trs31		C5	At5g58030	6	36.9	5	10.31	0.0018
Trs120	II	C9	At5g11040	44	44.1	6	9.99	0.0181
Trs20*	Shared	C2*	At1g80500[A]	2	20	7	8.55	0.0004
Bet5		C1	At1g51160	3	18.9	8	8.20	0.0036
Trs65*	III	C13*	At2g47960	8	26	10	7.33	0.0045
Trs85		C8	At5g16280	6	4.2	13	5.52	0.0265
-		C11*	At5g65950	8	9.6	16	5.26	0.0349
-		C12*	At4g39820	2	6.9	17	3.35	0.1837
Trs23	Shared	C4	At5g02280	-	-	-	-	-

Table I. Analysis of CLUB-GFP immunoprecipitates via label-free mass spectrometry.

Yeast and metazoan complexes are as described by Thomas et al. (2018) and Riedel et al. (2018). Shared subunits are colored in blue, TRAPPII-specific subunits in green and TRAPPIII-specific in orange. Flowers from transgenic plants were used (see experimental procedures). The data are based on intensity-based absolute quantification (iBAQ) values of the proteins in three biological replicates, with normalization to bait (see Supplemental methods). We imputed missing values with a constant value of 1000. AGI: Arabidopsis genome initiative accessions (www.arabidopsis.org). **-**: missing in the IP-MS data. *****: TRAPP subunit not previously recognised in plant genomes (see also Tables III to V). **A:** reannotation of TRAPPC2/C2L subunits, only one

of which has been previously described by Thellmann et al., 2010. **a**: overall number of unique peptides across the three experiments. **b**: The top ten proteins in the set of TRAPP subunits and RAB GTPases analyzed in this study are in bold; note that these are all shared or TRAPPII-specific components. **c**: The log2 intensity ratio for each protein was calculated from its average signal intensity in the experiment divided by its average intensity in the control, which was an empty soluble GFP vector. Detected TRAPP subunits were ranked according to their ratio between the experiment and negative control. The proteins are sorted by rank. Note that TRS65/TRAPPC13, which is a TRAPPII subunit in yeast but a TRAPPIII subunit in metazoans, had an intermediate intensity ratio of 7. 3 (see Fig. S1). The high confidence interactors include shared and TRAPPII-specific subunits. **d:** P values were calculated using the t-test (two-sided) and are all significant (P < 0.02) with the exception of those for TRAPPIII homologues, which are in red. This table lists only TRAPP components detected in the IPs.

Related to Fig. S1 on the CLUB interactome

Rab Clade	Rab GTPase	AGI	Peptides[a] unique (shared/razor + unique)	Sequence coverage %	Rank[b]	ratio[c]	P[d] =
E	E1a	At3g53610	1 (8)	41.7	**9**	7.6	1.26E-05
D	D2b	At5g47200	2 (9)	64.4	11	6.6	0.003
B	B1b	At4g35860	4 (4)	24.2	12	6.1	0.008
A	A2c	At3g46830	2 (4)	21.2	14	5.5	0.013
	A2a	At1g09630	1 (4)	19.8	15	5.4	0.007
G	G3f	At3g18820	-	-	-	-	-

Table II. Rab GTPases identified in CLUB/AtTRS130 IPs.

Flowers from transgenic plants were used. The data are based on intensity-based absolute quantification (iBAQ) values of the proteins in three biological replicates, with normalization to bait (see Supplemental methods). Flowers from transgenic plants were used (see experimental procedures). The data are based on intensity-based absolute quantification (iBAQ) values of the proteins in three biological replicates, with normalization to bait (see Supplemental methods). We imputed missing values with a constant value of 1000. AGI: Arabidopsis genome initiative accessions (www.arabidopsis.org). **a:** overall number of unique peptides across the three experiments; peptides in parentheses are shared/razor + unique. **b:** The top ten ranks in the set of proteins analyzed in this study are in bold. **c:** The log2 intensity ratio for each protein was calculated from its average signal intensity in the experiment divided by its average intensity in the control, which was an empty soluble GFP vector. Rab GTPases were ranked according to their ratio between the experiment and negative control. The proteins are sorted by rank of ratios. Note that all Rab-GTPases had intermediate intensities in our IP-MS data (intensity ratio in the 5 – 8 range). **d:** P values were calculated using the t-test (two-sided) and are all significant (P < 0.02). This table lists only Rab GTPases detected in the CLUB IPs.

Related to Fig. S1 on the CLUB interactome and Fig. S4 on RAB-A2a coverage and peptides in CLUB IPs.

TRAPP subunit			IP-MS values and statistics A2a WT/Col-0				
Yeast	Metazoan	AGI	Unique peptides	Sequence coverage %	rank[a]	Ratio[b] (log2)	P[c] =
YFP:RAB A2a (bait)		AT1G09630	38	95.9	**1**	21	-
Trs33	C6	AT3G05000	12	76.3	**3**	14	2.00E-07
Trs31	C5	AT5G58030	12	63.6	**4**	13	1.00E-06
Trs20*	C2*	At1g80500[A]	7	64.4	**5**	13	3.00E-08
Bet5	C1	AT1G51160	12	87.6	**6**	13	5.00E-07
Trs23	C4	At5g02280	8	62.4	**7**	12	3.00E-06
Tca17	C2L	At2g20930[A]	9	68.6	**8**	12	2.00E-07
Trs65*	C13*	At2g47960	22	64.7	10	12	4.00E-06
Bet3	C3	AT5G54750	12	54.8	11	12	8.00E-07
-	C12	At4g39820	26	72.1	12	11	2.00E-05
Trs120	C9	At5g11040	61	57.4	13	11	6.00E-05
YFP:RAB G3f		AT3G18820	26	93.2	16	10	7.00E-03
Trs85	C8	At5g16280	59	58.2	17	9	9.00E-03
-	C11*	At5g65950	48	52.2	18	8	3.00E-02
Trs130	C10	At5g54440	56	51.2	19	8	3.00E-02

Table III. TRAPP subunits identified in a differential IP-MS strategy using YFP: RAB-A2a GTPase as bait. Yeast and metazoan complexes are as described by Thomas et al. (2018) and Riedel et al. (2018). Shared subunits are colored in blue, TRAPPII-specific subunits in green and TRAPPIII-specific in orange. Microsomes isolated from roots were used. The data are based on intensity-based absolute quantification (iBAQ) values of the proteins in three biological replicates, with the exception of A2a-WT, for which we had six replicates. Normalization was to bait (see Supplemental methods). We imputed missing values with a constant value of 1000. **-:** missing in the IP-MS data. ***:** TRAPP subunit not previously recognised in plant genomes (see also Table I). **A:** reannotation of TRAPPC2/C2L subunits, only one of which has been previously described by Thellmann et al., 2010. **a:** The top nine proteins in the YFP:A2a IP-MS, within the set of proteins analyzed in this study, are in bold. **b:** The log2 intensity ratio for each protein was calculated from its average signal intensity in the experiment divided by its average intensity either in the control (wild-type Columbia microsomes). Detected TRAPP subunits and Rab GTPases were ranked according to their ratio between the experiment and negative control. The proteins are sorted by rank of ratios in the A2a-WT vs control experiment. **c:** P values were calculated using the t-test

(two-sided) and are all significant (P < 0.02), unless indicated in red. This table lists only TRAPP subunits detected in the IPs, as well as Rab GTPase bait proteins.

Related to Fig. S5 on YFP: RAB-A2a (WT) IP-MS.

TRAPP subunit		AGI	G3F/control			G3f-WT/ A2a-WT
Yeast	Metazoan		Rank[a]	Ratio[b] (log2)	P[c] =	Ratio (log2)[d]
YFP:RAB G3f (bait)		AT3G18820	**1**	21	-	12
YFP:RAB A2a		AT1G09630	**2**	14	3.00E-04	**-7**
Trs33	C6	AT3G05000	**4**	13	8.00E-04	**-1**
Trs31	C5	AT5G58030	**5**	12	1.00E-03	**-1**
Trs65*	C13*	At2g47960	**7**	12	2.00E-03	0
-	C12	At4g39820	**8**	12	9.00E-04	0
Trs20*	C2*	At1g80500[A]	**10**	11	3.00E-03	-2
-	C11*	At5g65950	11	11	1.00E-03	3
Trs85	C8	At5g16280	12	11	2.00E-03	2
Trs23	C4	At5g02280	13	11	9.00E-04	-2
Bet5	C1	AT1G51160	14	11	2.00E-03	-2
Tca17	C2L	At2g20930[A]	15	9	2.00E-03	-3
Bet3	C3	AT5G54750	16	9	1.00E-02	-2
Trs130	C10	At5g54440	17	8	2.00E-02	0
Trs120	C9	At5g11040	18	7	1.00E-02	-4

Table IV. TRAPP subunits identified in a differential IP-MS strategy using YFP: RAB-G3f GTPase as bait. Yeast and metazoan complexes are as described by Thomas et al. (2018) and Riedel et al. (2018). Shared subunits are colored in blue, TRAPPII-specific subunits in green and TRAPPIII-specific in orange. Microsomes isolated from roots were used. The data are based on intensity-based absolute quantification (iBAQ) values of the proteins in three biological replicates. Normalization was to bait (see Supplemental methods). We imputed missing values with a constant value of 1000. **-**: missing in the IP-MS data. *****: TRAPP subunit not previously recognised in plant genomes (see also Table I). **A:** reannotation of TRAPPC2/C2L subunits, only one of which has been previously described by Thellmann et al., 2010. **a:** The top ten proteins in the YFP:A2a IP-MS, within the set of proteins analyzed in this study, are in bold. **b:** The log2 intensity ratio for each protein was calculated from its average signal intensity in the experiment divided by its average intensity either in the control (wild-type Columbia microsomes). Detected TRAPP subunits and Rab GTPases were ranked according to their ratio between the experiment and negative control. The proteins are sorted by rank of ratios in the G3f-WT experiment vs Col-0 control. **c:** P values were

calculated using the t-test (two-sided) and are all significant (P < 0.02). **d:** Note that, in a pairwise comparison, shared and TRAPP-II specific subunits behave like the TGN/EE-localised RAB-A2a, whereas the TRAPPIII subunits (orange) behave like the vacuolar RAB-G3f. This table lists only TRAPP subunits detected in the IPs, as well as Rab GTPase bait proteins.

Related to Fig. 3 on YFP: RAB-G3f (WT) IP-MS.

TRAPP subunit		AGI	Rank			A2a-DN/control[b]		ratio[a] (log2)	
Yeast	Metazoan		A2a-WT	A2a-DN	A2a-CA	ratio[a] (log2)	P[c] =	A2a-DN/A2a-WT	A2a-DN/A2a-CA
YFP:RAB A2a (bait)		AT1G09630	**1**	**1**	**1**	21	-	0	0
Trs33	C6	AT3G05000	3	**2**	6	17	1E-04	3	9
Trs23	C4	At5g02280	7	**3**	2	17	3E-04	4	5
Tca17	C2L[A]	At2g20930[A]	8	**4**	8	16	3E-03	4	10
Bet5	C1	AT1G51160	6	**5**	7	16	7E-04	4	9
Trs31	C5	AT5G58030	4	**6**	5	16	1E-04	3	6
Trs20*	C2[A]	At1g80500[A]	5	**7**	4	16	2E-05	3	5
Bet3	C3	AT5G54750	11	**8**	19	15	5E-03	3	15
Trs120	C9	At5g11040	13	**9**	16	14	4E-03	3	11
Trs130	C10	At5g54440	19	**10**	18	8	2E-01	1	6
YFP:RAB G3f		AT3G18820	16	12	9	4	4E-01	-6	-2
Trs65*	C13*	At2g47960	10	-	10	-	-	-12	-6
Trs85	C8	At5g16280	12	-	13	-	-	-9	-3
-	C11*	At5g65950	18	-	15	-	-	-8	-3
-	C12	At4g39820	17	-	17	-	-	-11	-6

Table V. TRAPP subunits identified in a differential IP-MS strategy using YFP: RAB-A2a mutant variants as baits. Yeast and metazoan complexes are as described by Thomas et al. (2018) and Riedel et al. (2018). Shared subunits are colored in blue, TRAPPII-specific subunits in green and TRAPPIII-specific in orange. Microsomes isolated from roots were used. The data are based on intensity-based absolute quantification (iBAQ) values of the proteins in three biological replicates, with the exception of A2a-WT, for which we had six replicates. Normalization was to bait (see Supplemental methods). We imputed missing values with a constant value of 1000. **-**: missing in the IP-MS data. *****: TRAPP subunit not previously recognised in plant genomes (see also Table I). **A:** reannotation of TRAPPC2/C2L subunits, only one of which has been previously described by Thellmann et al., 2010. **a:** Detected TRAPP subunits and Rab GTPases were ranked according to their ratio between the experiment and negative control (wild-type Columbia microsomes). The proteins are sorted by rank of ratios in the A2a-DN vs. control experiment. **b:** The log2 intensity ratio for each protein was calculated from its average signal intensity in the experiment divided by its average intensity either in the control or in a different experiment. **c:** P values were calculated using the t-test (two-sided) and are all significant (P < 0.02), unless indicated in red. **d:** The top ten proteins in the YFP:A2a-SN IP-MS, within the set of proteins analyzed in this study, are in bold. Note that, in pairwise comparisons, shared and TRAPP-II specific subunits (green) have positive values, whereas the TRAPPIII subunits (orange) behave like the vacuolar RAB-G3f. This table lists only TRAPP subunits detected in the IPs, as well as Rab GTPase bait proteins.

Related to Fig. 3 on YFP: A2a-DN IP-MS.

Figure Legends

Figure 1. Binary interactions between TRAPP subunits.

(a). TRAPPII truncations used for binary interaction assays. Segments colored in red are conserved across kingdoms, while ones in green are plant-specific. The orange moiety of the C2 segment is poorly conserved across kingdoms. The T2 middle segment corresponds to sequences found to interact with the exocyst in a yeast two-hybrid screen (Rybak et al., 2014).

(b). Yeast two-hybrid experiments; the panels are spliced together from different plates. Four independent replicate experiments are shown. Note positive interactions between the plant specific C3_DB CLUB/AtTRS130 truncation and AtTRS120 T2_AD, and between CLUB C2_DB and T2_AD. A weak interaction was observed between TCA17_DB and C2_AD. T2_DB is an auto activator, as evidenced by colony growth with the empty AD vector, and this precludes our ability to determine whether AtTRS120_T2 interacts with any TRAPP subunit.

(c). A dimerization model best explains all the binary interactions reported here. This is based on the crystal structure of a core sub-complex (Kim et al., 2006) and on the TEM micrographs of the TRAPPII complex (YIP et al., 2010; Taussig et al, 2013). Arrows

represent the binary interactions in the DB to AD orientation and the thickness of the arrow depicts the strength of the interaction. Note that the TRS120-T3 truncation is included in TRS120-T2. TRAPPII-specific subunit segments coloured in red are conserved across kingdoms, while ones in green are plant-specific (see a.). Subunits common to TRAPPII and TRAPPIII are in blue. The pink asterisk depicts the approximate location of the putative GEF catalytic site, based on yeast models (Cai et al., 2008; Thomas et al., 2019).

Related to Fig. S2.

Figure 2. Double mutant analysis between *trs33-1* and *club-2.*

Embryogenesis in *trs33-1* and *club-2* single and double mutants. Null alleles were used for both loci. Asterisk points to the hypophysis or to its progeny. Black arrows: aberrant division plane. Blue arrow heads: aberrant cell shape. Note the aberrant cell division and deformed shape of *trs33-1 club-2* heart stage double mutants (bottom right panel). We detected 11% (n = 327) heart stage but 0% torpedo stage (n = 155 torpedo embryos in total; see Fig. S2) putative double mutant embryos from mother plants segregating both *trs33-1* and *club-2*. n = 157 embryos from 3 wild-type mother plants, n = 219 embryos from 3 *trs33-1* mother plants, n = 511 embryos from 6 *club-2* mother plants, n= 870 embryos from 7 *trs33-1 club-2* mother plants*.*

Related to Fig. S3

Figure 3. Volcano plots showing all co-purified proteins in YFP:RAB-G3f and YFP:RAB-A2a DN immunoprecipitates.

The ratio was calculated for each protein as the average intensity of the signal in the experiment divided by its average intensity in the negative Col-0 wild-type tissue. The P-value (depicted along a negative log10 scale) is plotted against the signal ratio. Dotted grey lines represent cutoffs: P-value < 0.02 and Ratio >8 or >5. The numbers in each field represent the total number of proteins detected with the respective P-value and ratio cutoff. **(a).** YFP:RAB-G3f vacuolar Rab GTPase bait (see Table IV). Note that TRAPPIII subunits (orange: TRAPPIII-specific subunits; blue: shared TRAPP subunits) cluster in the upper right quadrant, indicating high abundance and good reproducibility. TRAPPII-specific subunits (green) have a significant P-value but an intermediate intensity ratio.

(b). YFP:RAB-A2a DN bait (see Table V). Note that only TRAPPII subunits (green: TRAPPII-specific subunits; blue: shared TRAPP subunits) are in the upper right quadrant, indicating high abundance and good reproducibility. TRS130/CLUB is the only TRAPPII subunit that is not a high confidence interactor in the RAB-A2a IP-MS data. This is because it was also detected in the Col-0 non-transgenic control and hence did not meet our P-value cutoffs. TRAPPIII subunits (orange) are clustered in the lower left quadrant, which means that those proteins were not detected as A2a interaction partners in the A2a-DN mutant.

Related to Fig. S5 on YFP: RAB-A2a (WT) IP-MS.

Figure 4. Co-localisation of YFP:RAB-A2a with TRS120:mCherry and the behavior of YFP: RAB-A2a variants in *trappii* root tips. Live imaging with YFP marker in green and TRS120:mCherry/FM4-64 in magenta. Arrows point to cell plates and white-rimmed blue arrows to cross walls. Biogenesis, expansion and maturation refer to the cell plate at different cytokinesis stages (see experimental procedures). At least ten seedlings were imaged per marker line. Size bars = 5μm.

(a). Time-lapse of A2a$_{pro}$:YFP:RAB-A2a and UBQ$_{pro}$:TRS120:mCh, with minutes indicated in the right panel. YFP:RAB-A2a colocalizes with TRS120:mCh at the cell plate throughout cytokinesis, reorganizing to the leading edges (arrow heads) at the end of the cell cycle. Early and late stage time-lapses were imaged in two different cells. The numbers indicate minutes after the cell plate (arrow) becomes visible as a YFP:RAB-A2a and TRS120:mCh-positive compartment. n = 6 wild type cytokinetic cells.

(b)-(c). A2a$_{pro}$:YFP**:**RAB-A2a does not completely reorganize to the leading edges of the cell plate in *trappii* mutants. n = 35 cytokinetic cells for *club-2*; n = 20 cytokinetic cells for *trs120-4;* at least 20 seedlings were imaged per line.

(d-h). Sorting of YFP:RAB-A2a mutant (DN (GDP) or CA (GTP) bound) variants in *trs120-4* root tips.

(d). Ratio of signal intensity at the cell plate (CP) versus the plasma membrane (PM). This is significantly decreased for A2a$_{pro}$:YFP:A2a-DN (**: P < 0.01). Conversely, this is significantly increased for A2a$_{pro}$:YFP:A2a-CA (***: P < 0.00015). Cell cycle stage: anaphase to telophase transition.

(e)-(f). A2a$_{pro}$:YFP:A2a-DN (GDP-bound) does not fully reorganize to the leading edges of the cell plate in WT root tips. In *trs120-4* mutants, the signal is diffuse and cytosolic; it

labels aberrant endosomal compartments around the cell plate (yellow arrowheads) but not the cell plate itself. n = 15 wild type, n = 6 *trs120-4* cytokinetic cells.

(g-h). A2a$_{pro}$:YFP:A2a-CA (GTP-bound) weakly labels wild-type cell plates and ectopically localizes to the plasma membrane (red arrowheads). *trs120-4* mutants have a stronger YFP:A2a-CA signal at the cell plate, and a weaker plasma membrane localisation. n = 10 wild type, n = 17 *trs120-4* cytokinetic cells.
Related to Fig. S6 to S8.

Figure 5. TRAPP complexes and Rab GTPases in membrane trafficking.
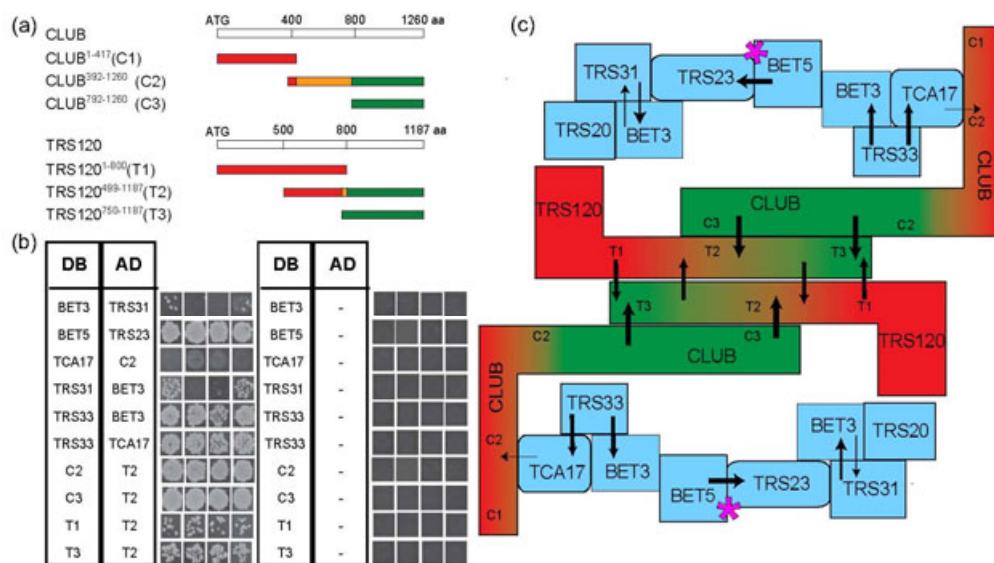
(a). Two TRAPP complexes are found in yeast: TRAPPIII acts as a GEF for Ypt1 and TRAPPII as a GEF for Ypt31/32 (Morozova et al., 2006; Thomas et al., 2018). TRAPPII acts at the TGN to mediate secretion and has also been implicated in autophagy (Thomas et al., 2018; Zou et al., 2013). TRAPPIII is involved in ER-Golgi traffic, in autophagy, and in trafficking between the medial/late Golgi and endosomes (Thomas et al., 2018). PAS: phagophore assembly site or pre-autophagosomal structure. The dashed arrow does not distinguish between medial/trans Golgi and the TGN and does not depict endosomes along post-Golgi trafficking routes.
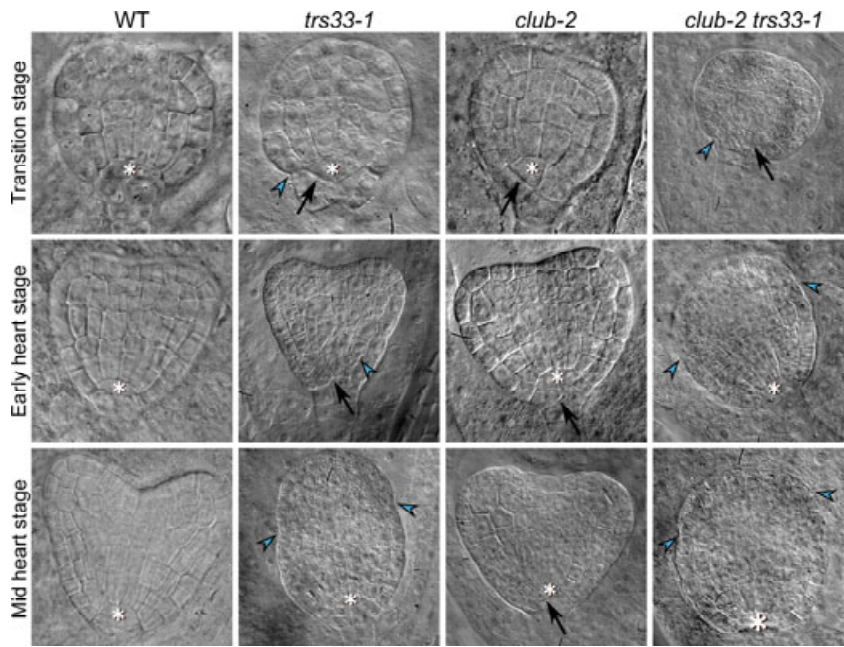
(b). Only two TRAPP complexes are known in metazoans. TRAPPII possesses GEF activity for both Rab-1 and Rab-11 (Riedel et al., 2018). Metazoan TRAPPIII possesses GEF activity for Rab-1 and is thought to play a role in ER-Golgi traffic, COPII recruitment to ER and autophagy (Scrivens et al., 2011; Bassik et al., 2013; Lamb et al., 2016; Zhao et al., 2017; reviewed by Sacher et al., 2018). The dashed arrow does not distinguish between medial/trans Golgi and the TGN and does not depict endosomes along post-Golgi trafficking routes.
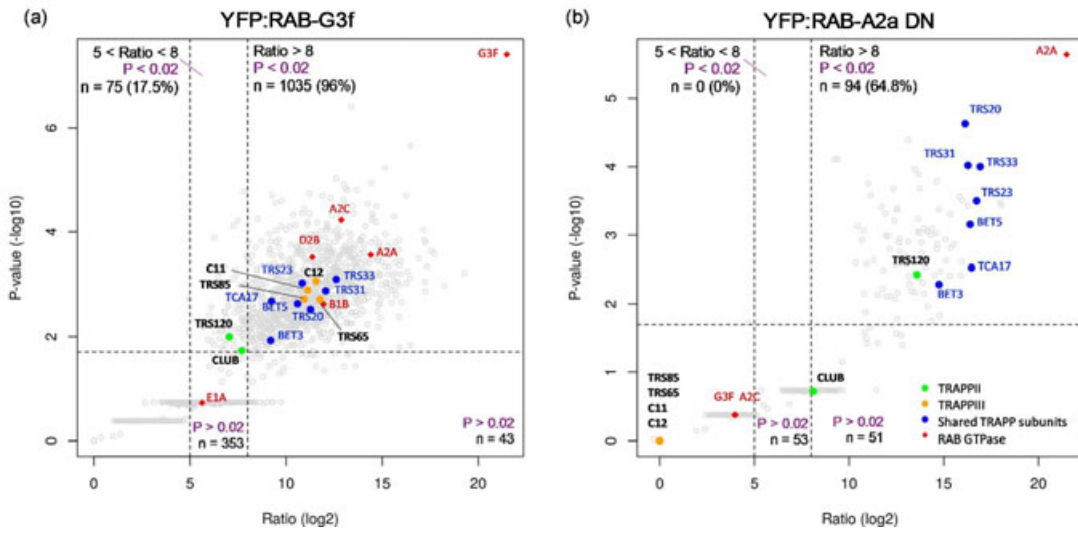
(c). In plants, TRAPPII resides at the TGN/EE and is a putative GEF for the Rab-A clade of Ypt3/Rab-11 orthologues. Rab clades identified in TRAPPII IP-MS are D, B, A and E and these are on a biosynthetic trafficking route. Rab-F or Rab-G clades were not robustly identified in the CLUB/AtTRS130 interactome. We postulate the existence of a plant TRAPPIII complex that resembles metazoan TRAPPIII. Based on preferential binding to the vacuolar Rab-G, which is required for autophagy (Kwon et al., 2013), and on orthology we tentatively place TRAPPIII on an autophagy and/or vacuolar trafficking route. Whether Arabidopsis TRAPPII or III play a role in ER-Golgi traffic remains to be

determined. The dashed arrow does not does not depict late endosomes/multivesicular bodies along post-Golgi trafficking routes.

RER: rough endoplasmic reticulum; TGN: trans-Golgi network; SV: secretory vesicles; CCV: clathrin coated vesicles.